

Received 21 September 2022, accepted 29 October 2022, date of publication 9 November 2022, date of current version 16 November 2022.

Digital Object Identifier 10.1109/ACCESS.2022.3221137

 SURVEY

# A Comprehensive Review of Lithium-Ion Batteries Modeling, and State of Health and Remaining Useful Lifetime Prediction

**MOHAMED ELMAHALLAWY<sup>ID</sup><sup>1</sup>, TAREK ELFOLY<sup>ID</sup><sup>1</sup>, (Senior Member, IEEE),**

**ALI ALOUANI<sup>1</sup>, (Senior Member, IEEE), AND**

**AHMED M. MASSOUD<sup>ID</sup><sup>2</sup>, (Senior Member, IEEE)**

<sup>1</sup>Department of Electrical and Computer Engineering, Tennessee Technological University, Cookeville, TN 38501, USA

<sup>2</sup>Department of Electrical Engineering, Qatar University, Doha, Qatar

Corresponding author: Tarek Elfouly (telfouly@tnstate.edu)

This work was supported by the Center for Energy Systems Research (CESR), Tennessee Technological University, Cookeville, TN, USA.

**ABSTRACT** According to the United States environmental protection agency (EPA), every burned gallon of gasoline generates 8.87 Kg of CO<sub>2</sub>. The pollution created by vehicles' fuel consumption has been one of the primary sources of environmental contamination that can lead to more climate changes and global warming. Thus, science and technology have converged on the idea that reducing fuel consumption benefits the environment and human health. One of the ideas for reducing fuel usage is deploying hybrid electric vehicles (HEVs) and electric vehicles (EVs) using renewable energy as alternatives to gasoline. One of the main issues with EV batteries is that over operational time the battery health degrades and ultimately becomes unsafe to use. It is crucial that safety issues be addressed by researchers and battery manufacturers. Assessing and predicting battery health has been a high-priority research topic to attempt to mitigate the danger introduced by EV batteries. Although various techniques have been developed to estimate and predict the battery's state of health (SOH), they do not cover all degradation scenarios that may affect the battery's lifetime. In addition, the models used in estimating and predicting the battery's lifetime need to be improved to provide a more accurate battery health state and guarantee battery safety while in use by an EV. Even though all types of EV batteries face similar issues, this paper focuses on *Li-ion* EV batteries. The main objectives of this paper are 1) to present various *Li-ion* battery models that are used to mimic battery dynamic behaviors, 2) to discuss the *degradation factors* that cause the battery lifespan to be degraded, and to become unsafe, 3) to provide a review of the *estimation and prediction techniques* used for Li-ion battery SOH and remaining useful life (RUL) estimation along with a discussion of their advantages and limitations, and 4) to provide recommendations for improving Li-ion battery lifetime estimation. This paper represents a concise source of information for battery community researchers to help expedite beneficial and practical outcomes to improve EV battery safety.

**INDEX TERMS** Electric vehicles (EVs), Lithium-ion (Li-ion) batteries, state of health (SOH), remaining useful life (RUL), battery models, battery aging.

## NOMENCLATURE

The next list describes several symbols that will be later used within the body of the Article

The associate editor coordinating the review of this manuscript and approving it for publication was Jie Gao <sup>ID</sup>.

<i>ANN</i>	Artificial Neural Network.
<i>BMS</i>	Battery Management System.
<i>BOL</i>	Beginning of Life.
<i>C-rate</i>	Charge/Discharge rate.
<i>CC</i>	Constant Current.
<i>CCCV</i>	Constant Current Constant Volt.

<i>CFNN</i>	Cascade Forward Neural Network.
<i>DOD</i>	Depth of Discharge.
<i>DVA</i>	Differential Voltage Analysis.
<i>EAM</i>	Electrode Average Model.
<i>ECM</i>	Equivalent Circuit Model.
<i>EIS</i>	Electrochemical Impedance Spectroscopy.
<i>ELM</i>	Extreme Learning Machine.
<i>EOL</i>	End of Life.
<i>EPA</i>	Environmental Protection Agency.
<i>ESN</i>	Echo State Network.
<i>EV</i>	Electric Vehicle.
<i>FFNN</i>	Feed Forward Neural Network.
<i>GPR</i>	Gaussian Process Regression.
<i>HEV</i>	Hybrid Electric Vehicle.
<i>HNN</i>	Hamming Neural Network.
<i>ICA</i>	Incremental Capacity Analysis.
<i>ITDNN</i>	Input Time-Delayed Neural Network.
<i>KSONN</i>	Kohonen Self Organizing Neural Network.
<i>LCA</i>	Lithium Cobalt oxide.
<i>LFP</i>	Lithium iron phosphate.
<i>Li-ion</i>	Lithium-ion.
<i>LSTM</i>	Long Short Term Memory.
<i>LTO</i>	Lithium Titanate Oxide.
<i>MAE</i>	Mean Absolute Error.
<i>ML</i>	Machine Learning.
<i>NAPCE</i>	NASA Ames Prognostics Center of Excellence.
<i>NARX</i>	Nonlinear Auto-Regressive with exogenous input.
<i>NCA</i>	Lithium Nickel Cobalt Aluminum oxide.
<i>NMC</i>	Lithium Nickel Manganese Cobalt oxide.
<i>ODE</i>	Ordinary Differential Equation.
<i>PDEs</i>	Partial Differential Equations.
<i>PDF</i>	Probability Density Function.
<i>PPM</i>	Porous electrode with Polynomial approximation Model.
<i>RBFNN</i>	Radial basis function Neural Network.
<i>RF/R</i>	Random Forest /Regression.
<i>RMSE</i>	Root Mean Square Error.
<i>RNN</i>	Recurrent Neural Network.
<i>ROEM</i>	Reduced-Order Electrochemical Model.
<i>RUL</i>	Remaining Useful Life.
<i>SDA</i>	Stacked Denoising Autoencoders.
<i>SEI</i>	Solid Electrolyte Interphase.
<i>SeM</i>	Semi-empirical Model.
<i>SOC</i>	State-of-Charge.
<i>SOH</i>	State-of-Health.
<i>SPM</i>	Single Particle Model.
<i>SPMe</i>	Single Particle Model with electrolyte.
<i>SVM</i>	Support Vector Machine.
<i>SVR</i>	support vector regression.
<i>USABC</i>	United States Advanced Battery Consortium.
<i>V<sub>oc</sub></i>	Open Circuit Voltage.

## I. INTRODUCTION

Environmental issues caused by Gasoline-powered vehicles are a challenge to automotive manufacturers worldwide. Global energy policies that stress low-carbon emissions require transforming and upgrading vehicles to use environmentally-friendly renewable energy sources. Lithium-ion (Li-ion) batteries are commonly used as an energy source in electric vehicles (EVs) and hybrid electric vehicles (HEVs) [1], [2] due to their relatively high energy density as well as their fast charging and low self-discharge rate [3]. As a point of clarification, in this paper, we refer to a single battery cell as a battery, whereas an EV's entire battery is referred to as a battery pack unless otherwise stated. Batteries' performance degrades over time and usage due to power fading and capacity loss [4]. This phenomenon is called battery aging, which occurs due to factors impacting battery performance, including chemistry degradation, manufacturing issues, atmospheric conditions (low/high temperature), and operational conditions. Two parameters describe the age of batteries: beginning-of-life (BOL), when the battery is first used, and end-of-life (EOL), when the battery is no longer usable. A battery capacity measures the available energy that the battery can deliver. It is proportional to the usable lithium inside the battery. The diagnosis and prognosis for Li-ion battery health are essential to guarantee safety while batteries are in operation. The battery state-of-health (SOH) estimation and/or remaining useful life (RUL) prediction are used to track and monitor its age. The battery SOH is defined as the ratio of the battery current capacity to its capacity at BOL, whereas the battery RUL is defined as the remaining battery life to reach its EOL. It is worth noting that the remaining battery life can be measured either as a calendar age (years or months) or as a cycling age (number of remaining cycles). In applications like EVs, where the amount of energy available in the battery plays an important role, the battery's capacity is often considered when measuring the battery age [4], [5]. In contrast, for applications where power is an essential issue, such as in HEVs, the change in the internal resistance is usually measured as a SOH metric [4], [5]. Generally, the battery reaches its EOL when its capacity drops to (70-80)% of its initial value at the BOL or when its internal resistance doubles [5].

Battery aging impacts both the state-of-safety (SOS) and the performance of EVs as it decreases the vehicle's response to accelerating and reduces the driving range. The SOS is affected by many events. For example, if the battery's internal resistance increases beyond a certain limit, the thermal heat released from the battery will also increase and can cause a fire that can lead to loss of life [7]. Table 1 shows some examples of EV-related fire incidents that occurred in the past few years with various scenarios, including parked vehicles (unplugged), crashed vehicles, or simply within driving or charging operations. In addition, Figure 1 illustrates an example of what happened to the EVs' battery pack after a fire.

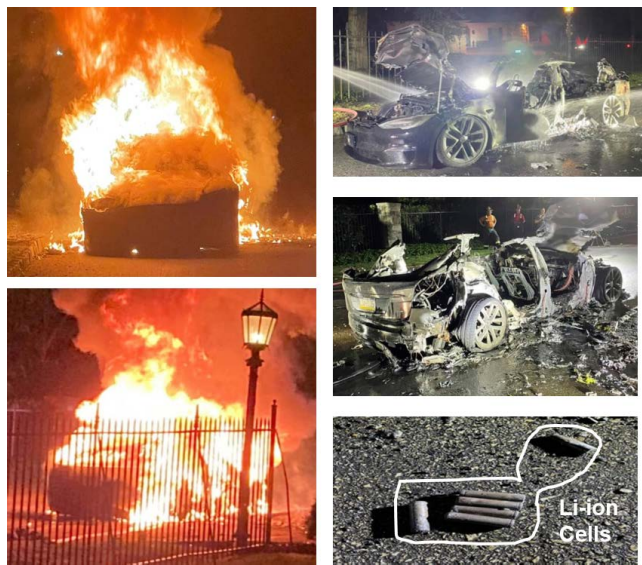


**FIGURE 1.** An example of an electric vehicle caught fire [6].

**TABLE 1.** List of selective EVs fire incidents for various scenarios.

Incident scenario	Incident date	Incident location
Fire while being parked (Unplugged)	Mar.2019 [8]	Tilburg, Netherlands
	Jul.2020 [9]	Virginia, USA
	May.2021 [10]	Ashburn, Virginia, USA
	Jun.2021 [11]	Boryeong, South Korea
Fire while being charged	Mar.2019 [9]	Massachusetts, USA
	Oct.2020 [12]	Lucie, Florida, USA
	Oct.2020 [13]	Gyeonggi-do, South Korea
	Nov.2020 [14]	Langenfeld, Germany
Fire while being driven	May.2018 [15]	Hubei, China
	Jun.2018 [7]	California, USA
	Jun.2021 [6]	Haverford, Pennsylvania
	Jul.2021 [16]	California, USA
Fire after vehicle crashed	Mar.2018 [7]	Texas, USA
	May.2018 [17]	Florida, USA
	May.2018 [18]	Ticino, Switzerland
	Apr.2021 [19]	Texas, USA

The capacity of a Li-ion battery can be directly measured using the coulomb counting method under galvanostatic charging/discharging. A battery's available capacity is generally measured by how much current passes through it over time until it is discharged. A battery state-of-charge (SOC) is the ratio between the available capacity of a battery and the maximum possible charge it can store. Capacitance is also commonly used to determine the SOH of a battery.

To better understand Li-ion battery dynamics, researchers have developed a variety of battery models. For example, an electrochemical battery model that describes the battery's internal chemical parameters, such as lithium concentration in both the positive and negative electrodes, kinetic

energy within the battery, and charge transfer, is developed to estimate the SOH and/or to predict the RUL. The model comprises a set of partial differential equations and requires the knowledge of several parameters. The full order of the electrochemical model cannot be used in real-time for battery health estimation [20], [21]. Thus, if these unknown parameters are inaccurately identified, this model will lose its advantage of accurately estimating the battery SOH. Researchers developed alternative models to estimate battery SOH, such as the equivalent circuit models (ECMs). ECMs use capacitors and resistors-based circuits to study battery dynamics using different input currents [22]. In addition, several reduced-order models of the full-order electrochemical model were considered with some assumptions to estimate battery SOH using adaptive filters, such as Kalman filters and particle filters [23], [24]. Moreover, several review papers estimating and predicting battery health based on the aforementioned models have been published [25], [26], [27], [28], [29].

Recently, researchers and industrial sectors have become increasingly interested in data-driven models for battery health diagnosis and prognosis due to their flexibility and the fact that they do not require any knowledge of the physical or chemical properties of the batteries, making them *model-free models*. Model-free means treating the battery as a black box with inputs and outputs, where the inputs are extracted from the training data. Based on the inputs, data-driven models are used to determine the battery SOH and predict its corresponding RUL. These models require extensive datasets to accurately estimate and predict battery health. The effectiveness of these models is greatly affected by the quality and quantity of collected data used for the training and testing processes.

Several technologies can facilitate the building of data-driven models, including differential analysis methods, empirical and data-fitting techniques, and machine learning (ML) algorithms. Differential analysis models are based on the relationship between the battery SOH and its thermal, electrical, and mechanical behaviors [30]. In addition, the differential models use voltage, surface temperature, and strain information to determine the effect of aging on battery SOH estimation [31]. Empirical and data fitting techniques are used to fit large amounts of data collected based on certain conditions to estimate battery SOH by assuming similar operational conditions and high computational efficiency. Nowadays, ML models have become increasingly popular in estimating and predicting battery SOH. This is due to ML flexibility and the ability in nonlinear mapping between inputs and outputs. To estimate the SOH or prediction of the RUL, relevant data, such as battery output voltage and charging current should be collected throughout battery operation and mapped to the battery SOH. Data-driven modeling tends to focus on either estimating batteries' SOH or predicting their RUL [32], [33], [34], [35], [36]. Therefore, research addressing both aspects (battery SOH/RUL) is needed since SOH is used as an input to the RUL predictors. However, SOH and RUL are discussed and reviewed in [37], [32],

and [38], and data-driven models used in EV applications are not comprehensively covered and not sufficiently compared to other diagnostic and prognostic techniques.

### The main contributions of this article are as follows:

- Provide an overview of the battery operation, characteristics, and degradation factors. In addition, we present a detailed review of various Li-ion battery models that mimic batteries' dynamic behavior.
- Review and identify the merits and challenges of several battery health estimations and prediction methods for various battery models.
- Analyze in-depth the data-driven models for estimation and prediction of battery health, focusing on the ML models.
- Discuss the strengths and weaknesses of each ML model and provide suggestions on overcoming these models' shortcomings for better accuracy of battery lifetime estimation and prediction.

The rest of this paper is organized as follows: Section II discusses the Li-ion battery charging and discharging operations. The characterization parameters of Li-ion batteries, such as power capacity, battery internal impedance, and open-circuit voltage, are presented in Section III. In Section IV, an overview of Li-ion battery models is discussed. The aging factors affecting the Li-ion battery lifetime are comprehensively surveyed in Section V. The battery SOH estimation methods are discussed and compared in Section VI concerning their advantages and disadvantages, along with suggested ideas for improving battery lifetime estimation. In section VII, various RUL prediction techniques, including the electrochemical prediction methods and data-driven methods are explained in detail. The performance evaluation of various RUL prediction techniques is compared in Section VIII. Section IX presents the limitations of the current models and some enhancement ideas for SOH estimation and RUL prediction. Finally, the work is concluded in Section X.

## II. LI-ION BATTERY OPERATION

Li-ion batteries are prevalent due to their high energy density. Consequently, these batteries can be used in high-energy applications, such as EVs. This section discusses how the

Li-ion battery operates during the charging and discharging phases. In EVs, the battery pack comprises several modules, each containing up to hundreds of batteries. Figure 2 illustrates the charging and discharging processes of each Li-ion battery. In general, each battery consists of two electrodes (positive and negative) with a separation region between them. The anode is considered a negative electrode, whereas the cathode is considered a positive electrode, and the separator between them is fabricated using porous material. Once the electrodes are placed, the remaining distance between the separator and the electrode is filled with liquid electrolyte.

Typically, Li-ion batteries contain lithium-metal oxide (which performs better than lithium) due to their ability to intercalate. Different lithium-metal oxides, used as a cathode electrode, are presented in Figure 3. In the automotive industry, NCA is a good choice because of its long lifetime, high specific energy storage, high power density, low cost, and high safety [39]. In contrast, the anode electrode uses lithium-carbon compounds (graphite). For instance, as shown in Figure 2, the cathode electrode uses lithium-metal oxide (i.e., LCA), whereas the anode electrode uses Li-Carbon. Generally, the electrons flow according to redox reactions, which can be divided into two categories. The former is called oxidation half-reaction, which happens when the anode emits electrons. The latter is called a reduction half-reaction that happens when electrons are taken up by the cathode. Detailed information about the charging and discharging processes inside Li-ion batteries can be found in the following subsections.

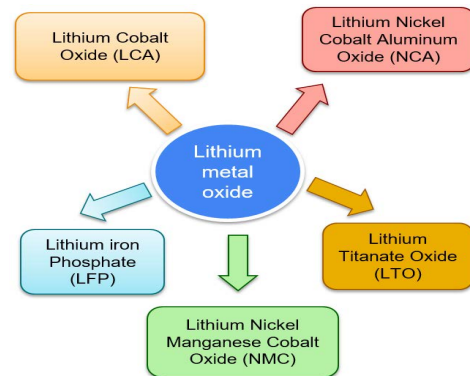


**FIGURE 3.** Different types of lithium metal oxide.

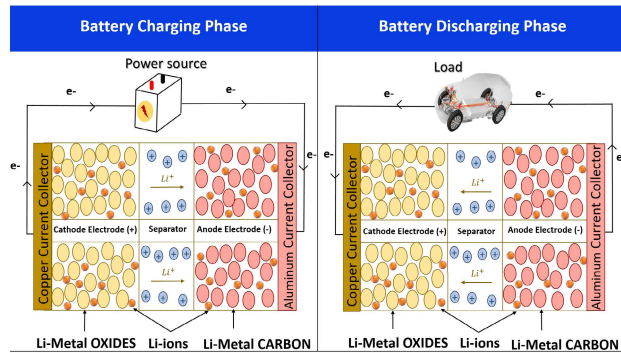


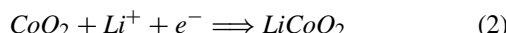
**FIGURE 2.** Charging and discharging processes of a Li-ion battery.

Once the battery reaches its maximum storage capacity, the oxidation process is completed.

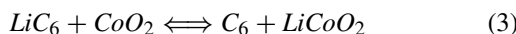


### B. DISCHARGING PHASE

The battery begins to discharge when an electrical load is connected between its terminals. Equation 2 depicts how the load consumes energy, which considers the reverse operation of the charging process [40]. The discharging process involves moving the positively charged lithium ions ( $Li^+$ ) from a negative electrode (anode) to a positive electrode (cathode). Therefore, electrons will be transferred from the cathode to the anode.



The charge and discharge processes of Li-ion batteries can be repeated up to thousands of times until the battery reaches 70-80% of its maximum capacity, defined previously as the battery EOL. At that time, it becomes retired and starts its second life. Equation 3 summarizes the oxidation-reduction reactions of a Li-ion battery.



## III. LI-ION BATTERY CHARACTERIZATION

Understanding the Li-ion battery characteristics under all operating conditions is vital for achieving the highest energy level and cost-efficiency. In this section, the characteristics that describe Li-ion battery behaviors will be discussed, which are used as standard benchmarks for estimating the SOC and SOH of the battery. The Li-ion battery is characterized by three main dynamic parameters: 1) power capacity, 2) battery internal impedance, and 3) open-circuit voltage ( $V_{oc}$ ). The battery's internal impedance and open-circuit voltage are affected by temperature and operating conditions.

### A. POWER CAPACITY

The power capacity is typically defined as how much electric charge can be stored inside a battery. Therefore, the capacity can be directly measured by integrating the current during the charging process. This direct measurement method counts the amount of charge, so it is called *coulomb counting*, and it can be expressed mathematically as follows:

$$C_{bat} = \int_0^t i \, dt \quad (4)$$

where  $C_{bat}$  denotes the battery capacity,  $i$  is the charging current, and  $t$  is the time required for the battery to be fully charged. Additionally, the battery SOC, which determines the capacity level based on input current, can directly be measured by coulomb counting as:

$$SOC_{bat}(t) = SOC_{batt}(t_0) + \frac{1}{C_{nominal}} \int_{t_0}^{t_n} i \, dt \quad (5)$$

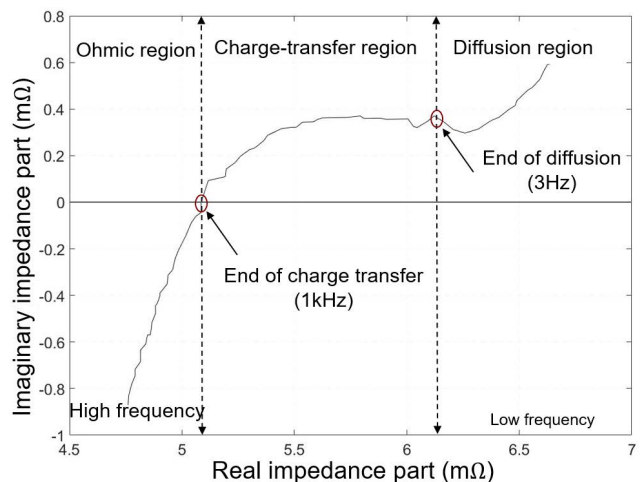


**FIGURE 4.** Nyquist plot of EIS spectrum for Li-ion battery internal impedance.

where  $SOC_{bat}(t)$  is the SOC of the battery at any time  $t$ ,  $SOC_{batt}(t_0)$  is the initial SOC of the battery at the beginning,  $C_{nominal}$  is the nominal capacity, and  $t_0, t_n$  are the initial and the final time for the battery to be full charged/discharged, respectively.

Different charge/discharge methods are usually employed to measure Li-ion battery capacity, such as constant-current constant-voltage (CCCV) discharge [41] or a constant discharge current pulse [42]. An alternative method is to apply a constant voltage until the current reaches a preset value during discharge. The relationship between the rate of charge or discharge currents and the nominal battery capacity defines as the C-rate.

### B. BATTERY INTERNAL IMPEDANCE

The battery's internal impedance is essential to determine its age. The battery RUL decreases as the impedance of the battery increases. Various methods have been developed to measure the battery's internal impedance. One of the popular methods for measuring the battery's internal impedance is electrochemical impedance spectroscopy (EIS), which can be expressed as a function of frequency between kHz and MHz. A battery's EIS spectrum can be determined experimentally when discharging it by applying low current levels as input while measuring  $V_{oc}$  as output and capacitive effects as positive phase angles. In EIS, the spectrum (Nyquist frequency) plot is a valuable diagnostic tool for presenting differences in frequency range as a function of battery SOC [40].

Figure 4 illustrates a typical EIS plot of a battery's frequency versus internal impedance. According to this figure, the battery's impedance is pure ohmic at high frequency, but the impedance becomes capacitive at low frequency, representing the charge transfer and diffusion regions. It should be noted that the battery has to be replaced if the internal impedance doubles [5]. Although EIS provides valuable insights, it cannot be used while the battery is in operation.

### C. OPEN CIRCUIT VOLTAGE

The open-circuit voltage  $V_{oc}$  is a fundamental battery characteristic because it helps estimate the battery SOH. Additionally, the measure of  $V_{oc}$  plays an important role in developing the electrical models that are used in estimating battery life. In most research studies, the battery behavior is predicted and modeled using  $V_{oc}(\text{SOC})$  dependency [43]. However, temperature impacts the estimation of  $V_{oc}(\text{SOC})$ .

The characterization of  $V_{oc}$  is usually carried out using various methods. One of these methods is the galvanostatic intermittent titration technique (GITT). This method applies a constant charging or discharging current until the appropriate SOC is reached. After that, it permits the battery to relax for a certain time to enhance its stabilization [44]. Conversely, the relaxation time and  $\Delta \text{SOC}(\%)$  influence the required time for the test to be done. For instance, in the case of a high precision  $\Delta \text{SOC}$  of 5% at charge rate 1C followed by a relaxation time of 40 hours, the battery test may take several months for only one cycle [44].

### IV. LI-ION BATTERY MODELS

Several models have been developed to mimic the dynamic behaviors of Li-ion batteries, each with a different level of accuracy and complexity. As shown in Figure 5, these models can be classified into four categories. The main objective of developing these models is to estimate battery SOH and predict battery RUL. In addition, these models can help improve the design and optimize the performance of the battery management systems (BMSs) in controlling the battery pack of EVs. Generally, the choice of the appropriate battery model is influenced by the application it is used for and the level of estimation accuracy required. Besides the models presented in Figure 5, there are other battery models, such as kinetic battery models, which represent batteries with two tanks (one for available energy and another for bound energy), and several others that are particularly suitable for lead-acid batteries. However, they are out of the scope of this paper.

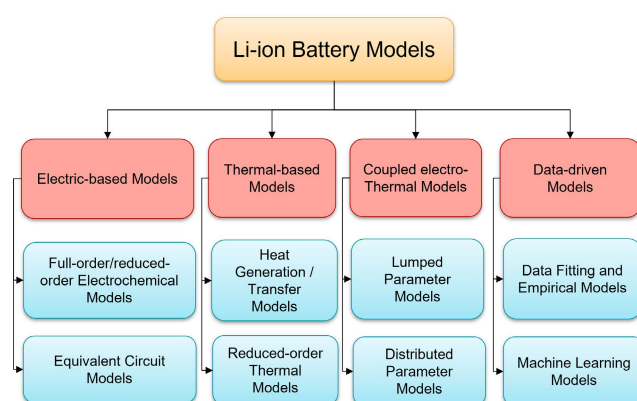


**FIGURE 5.** Classification of Li-ion battery models.

### A. ELECTRIC-BASED MODELS

Electric-based models primarily include full-order electrochemical models [45], reduced-order electrochemical models (ROEMs) [46], [47], and equivalent circuit models (ECMs) [48], [49]. Doyle et al. [45] proposed the full-order electrochemical model (white box model or physical model), which is known as a pseudo-two-dimensional (P2D) model to explain battery dynamic behavior with a variety of polymeric separator materials, composite cathodes, and lithium salts. The P2D model is expressed on a macro x-scale along the thickness of the positive and negative electrodes, and another micro r-scale along the direction of the solid-phase electrode particles. Due to this two-dimensional representation, this model is referred to as a pseudo-two-dimensional model. It is worth noting that each electrode is made up of many microscopic particles, and each particle is like a rice ball with many grains [50]. The structure and chemistry of the particles determine how well the battery operates. The major advantage of the full-order electrochemical model is its ability to accurately depict the chemical reactions and the battery's dynamic behavior, including lithium concentration in solid and electrolyte phases, lithium diffusion, and electric potential. In real-time applications, however, it is nearly impossible to determine many battery parameters related to chemical compositions, where the full-order electrochemical model requires solving a set of partial differential equations (PDEs) [21]. The measurement of some of these parameters is not directly available or even possible, and other parameters change with the aging of batteries over time. Under certain assumptions, the full-order electrochemical model can be simplified to reduce its complexity to be suitable for real-time applications. For this purpose, different ROEMs have been developed [51], [52], [53], [54], [55], [56], [57], [58]. In Table 2, the P2D model and some of the available ROEMs are compared with respect to their assumptions, advantages, and limitations.

Based on the input-output characteristics of the Li-ion battery, the ECMs were developed using electric circuit ele-

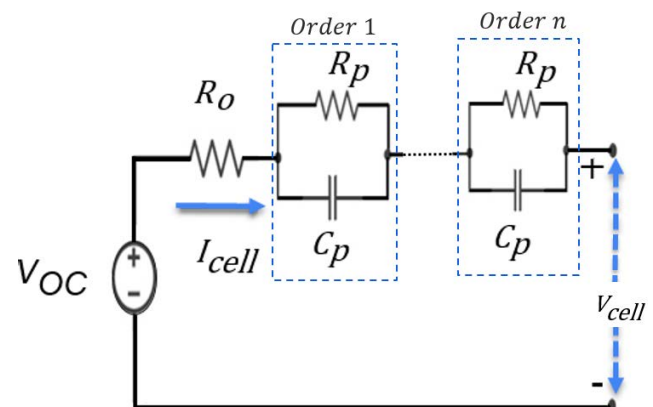


**FIGURE 6.** Equivalent circuit model of Li-ion battery of  $n$  R-C networks.

**TABLE 2.** Comparison of various electrochemical battery models.

Model	Assumption	advantages	Remarks
P2D Model [45, 59, 60]	<ul style="list-style-type: none"> <li>• Solid phase <math>\Rightarrow</math> multiple identical spherical particles</li> <li>• Electrolyte phase&amp; potentials <math>\Rightarrow</math> varying in <math>x</math> direction</li> <li>• Diffusion is considered in <math>r</math> direction</li> </ul>	<ul style="list-style-type: none"> <li>• Describes the entire electrochemical process during battery operation</li> <li>• Describes battery dynamics over space and time</li> <li>• High accuracy to estimate battery SOH</li> </ul>	<ul style="list-style-type: none"> <li>• Requires a significant amount of parameters</li> </ul>
Electrode Average Model (EAM) [51]	<ul style="list-style-type: none"> <li>• Neglects solid phase concentration</li> <li>• Considers only electrolyte phase concentration</li> <li>• Electrolyte phase concentration <math>\Rightarrow</math> battery SOC</li> </ul>	<ul style="list-style-type: none"> <li>• Very simple to set-up (few parameters)</li> <li>• Estimates battery SOC with high degree of accuracy</li> </ul>	<ul style="list-style-type: none"> <li>• Big error in voltage prediction</li> <li>• Heavy loss of information</li> <li>• Parameter identification is hard for real-time applications</li> </ul>
Porous electrode with Polynomial Model (PPM) [54]	<ul style="list-style-type: none"> <li>• Parabolic profile describes each spherical particle</li> <li>• Incorporates the parabolic approximation with the P2D model</li> </ul>	<ul style="list-style-type: none"> <li>• Estimates the battery voltage at higher discharge rates (<math>\geq 1C</math>)</li> <li>• Voltage prediction error <math>\in 0.013\text{--}0.135\%</math> <math>\rightarrow</math> discharge rate = <math>2C</math></li> </ul>	<ul style="list-style-type: none"> <li>• Similar complexity to other porous electrode models</li> </ul>
Single Particle Model (SPM) [52–54]	<ul style="list-style-type: none"> <li>• Each electrode <math>\Rightarrow</math> single spherical particle</li> <li>• Neglects electrolyte phase concentration</li> <li>• PDEs of solid phase concentration is simplified to be ODEs</li> </ul>	<ul style="list-style-type: none"> <li>• Battery's voltage estimation accuracy is high at low discharge rates (<math>&lt; 1C</math>)</li> <li>• Voltage prediction error <math>\in 3.404\text{--}6.70\%</math> <math>\rightarrow</math> discharge rate = <math>1C</math></li> </ul>	<ul style="list-style-type: none"> <li>• Inaccurate at high discharge rate (<math>\geq 1C</math>)</li> <li>• Voltage prediction error <math>\in 59.37\text{--}67.43\%</math> <math>\rightarrow</math> discharge rate = <math>2C</math></li> </ul>
SPM with electrolyte (SPMe) [55]	<ul style="list-style-type: none"> <li>• Same assumptions of SPM</li> <li>• Considers concentration of electrolyte phase</li> </ul>	<ul style="list-style-type: none"> <li>• More accurate at high discharge rates</li> <li>• Voltage prediction error <math>\in 19\text{ mV}</math> <math>\rightarrow</math> discharge rate = <math>5C</math></li> </ul>	<ul style="list-style-type: none"> <li>• More complex compared to the traditional SPM</li> </ul>

**Note:** SPM is considered the most reliable model, so many efforts are being made to improve its accuracy in predicting battery voltage by considering degradation factors and thermal dynamics under different charge/discharge conditions such as mechanical stress [56–58]

ments (resistance, capacitance, and voltage source). ECMs are widely used because they are simple to build and have a limited number of parameters that can be identified for onboard applications. Figure 6 shows the general framework of ECMs with  $n$  different RC networks. In Figure 6, the resistance  $R_0$  represents the ohmic resistance of the Li-ion battery, whereas the RC networks represent the polarization characteristics and diffusion effects of both electrodes. The model order is determined by the number of RC networks used, which must be selected carefully for an accurate estimation of battery voltage. For instance, Rui et al. [22] examined the accuracy of voltage estimation ( $V_{cell}$ ) at different orders of RC networks. Furthermore, a number of studies have reported that the first-order and second-order ECMs are sufficient to represent battery dynamics for EV applications, whereas higher-order models are not always the best choice in many scenarios [61].

### B. THERMAL-BASED MODELS

Battery temperature is another crucial aspect of the BMS of EVs since it affects battery performance and its lifetime [21]. The thermal behavior of batteries is better understood by developing several models, such as heat transfer, heat generation, and reduced-order thermal models. Different models of heat generation in batteries were developed to describe ohmic losses, activation, and concentration, resulting in a non-uniform distribution of heat inside the battery. The equations describing the various sources of heat generation and heat convection produced by Li-ion batteries can be found in [21], [62], and [63]. To make the full-order heat

generation models suitable for onboard battery applications, various reduced-order thermal models were developed to estimate/control the temperature of batteries [64], [65]. For instance, Kim et al. [64] proposed a reduced-order thermal model to estimate the battery's internal temperature. The proposed model is based on two assumptions: 1) the battery volume is homogeneous and isotropic, and 2) there is no rapid change in the temperature of the cooling media. Based on these assumptions, they modeled the thermal properties of the battery using volume averaging of the temperature gradient. The dual Kalman filter is used to estimate the core temperature of the battery based on its surface temperature. This filter combines two different Kalman filters, the traditional Kalman filter, and the extended Kalman filter.

### C. COUPLED ELECTRO-THERMAL MODELS

There is a strong correlation between batteries' electric and thermal behavior, which motivated researchers to develop battery models based on these relationships. Several coupled electro-thermal models have been proposed to describe the electrical and thermal properties of Li-ion batteries, simultaneously [66], [67]; including lumped-parameter and distributed-parameter models [21], [68]. Chiew et al. [68] developed a three-dimensional electrochemical-thermal coupled model for a Li-Iron Phosphate battery to include the thermal properties of such batteries during discharge. This coupled model incorporates an electrochemical model and a three-dimensional lumped thermal model to describe the temperature dynamics to compute the battery SOC. They validated their model experimentally on 26,650 cylindrical LFP batteries to demonstrate that the battery can perform

differently at a lower ambient temperature and discharge rate where more mild exothermic reactions occur. Their simulations show that for a lower discharge rate at 1C, the temperature gradient and heat produced by the battery are lower than those produced at higher discharge rates of 2C-4C. Hariharan et al. [21] also developed a coupled three-dimensional electro-thermal model to evaluate the effects of battery dynamics, such as the flow rate of liquid coolant and discharge current.

#### D. DATA-DRIVEN MODELS

Data-driven models are intelligent algorithms for finding a mapping between inputs and outputs by considering the battery as a black box. In batteries, voltage, current, and temperature are the most widely used input features, whereas the output is the battery SOC or SOH. A variety of data-driven models, including neural networks [69], [70], [71], long-short term memory(LSTM) methods [72] and support vector machines (SVMs) [38], [73], have been developed to describe battery behavior without prior knowledge of battery physics or chemistry. Data-driven models perform well when sufficient and high-quality datasets are used for developing a battery model. Thus, a dataset must accurately represent a battery operation at different ages under different operational conditions. Details regarding data-driven models will be discussed later in Section VI-A and SectionVII-B.

#### V. AGING FACTORS OF LI-ION BATTERY

Various aging factors influence Li-ion batteries' lifetime, including thermal, electrical, and mechanical abuse. Monitoring these aging factors is necessary to keep track of changes in the electrochemical degradation parameters, including the SEI layer growth and decomposition, the electrolyte decomposition, the graphite exfoliation, and other battery degradation parameters that directly impact capacity or power. In many studies, SEI layer growth is noted as one of the most important electrochemical degradation parameters that influence battery health [4]. More specifically, the change in the SEI layer thickness highly affects the battery's capacity. Figure 7 shows the various battery aging factors that may cause the battery pack of EVs to catch fire under various scenarios, including overheating or overcharging, as well as vehicle accidents. As a result of these aging factors that affect Li-ion batteries, researchers have been motivated to find a solution able to accurately predict the battery SOH. Consequently, understanding how each aging factor impacts a battery's behavior will assist in improving its performance and preventing/mitigating the occurrence of such types of abuses. An illustration of the impact of these aging factors on battery parameters is shown in Figure 8. The failure of the EV's battery pack may occur if only one battery (i.e., cell) is affected by one or more of these aging factors.

#### A. THERMAL ABUSE

Thermal abuse describes the impact of temperature change on the different components of a battery. In Li-ion batteries, the

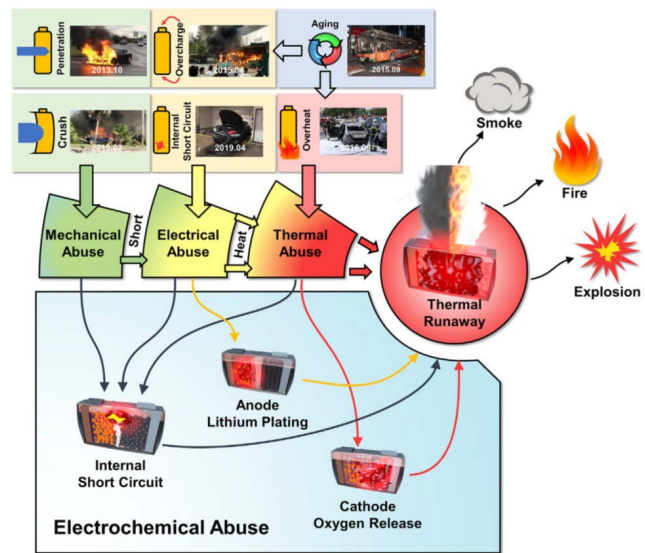


**FIGURE 7.** Various scenarios that may lead to Li-ion battery thermal runaway [74].

temperature change is due to chemical reactions inside the battery. In addition, the ambient temperature highly affects the performance of the battery. The relationship between chemical reactions and temperature follows the Arrhenius equation during the charge and discharge processes of the battery. According to thermodynamic definitions, these chemical reactions can be categorized into *endothermic reactions*, and *exothermic reactions*. When Li-ion batteries are being charged, they produce exothermic heat, which generates excessive heat from chemical reactions, dissipating easily into the environment. Alternatively, when the battery is fully charged, the reaction can be endothermic because the battery absorbs heat from its surroundings. The temperature gradient can also affect the ionic conductivity of electrodes and electrolytes, significantly shortening the battery's lifespan. As a result, Li-ion batteries used in EVs are unlikely to meet the expectations of a 10-year lifetime. Furthermore, the temperature does not only affect the battery's lifespan but could also cause thermal runaway issues, which affects the battery SOH.

#### 1) LOW-TEMPERATURE EFFECT

The ability of a cooling system to decrease the battery's ambient temperature to be below the level ( $0^{\circ}\text{C}$ ) affects its performance [76]. Due to the different properties of the materials used in a battery, the battery's performance may be degraded at low temperatures (*under-zero temperatures*). It is possible to classify the effects of low temperatures on performance into three classes: 1) change in electrolyte viscosity 2) change in charge transfer resistance 3) impact on Li-plating (when metallic lithium forms around the anode during charging).

Firstly, a decreased temperature results in a greater increase in the electrolyte viscosity, which decreases the electrolyte's

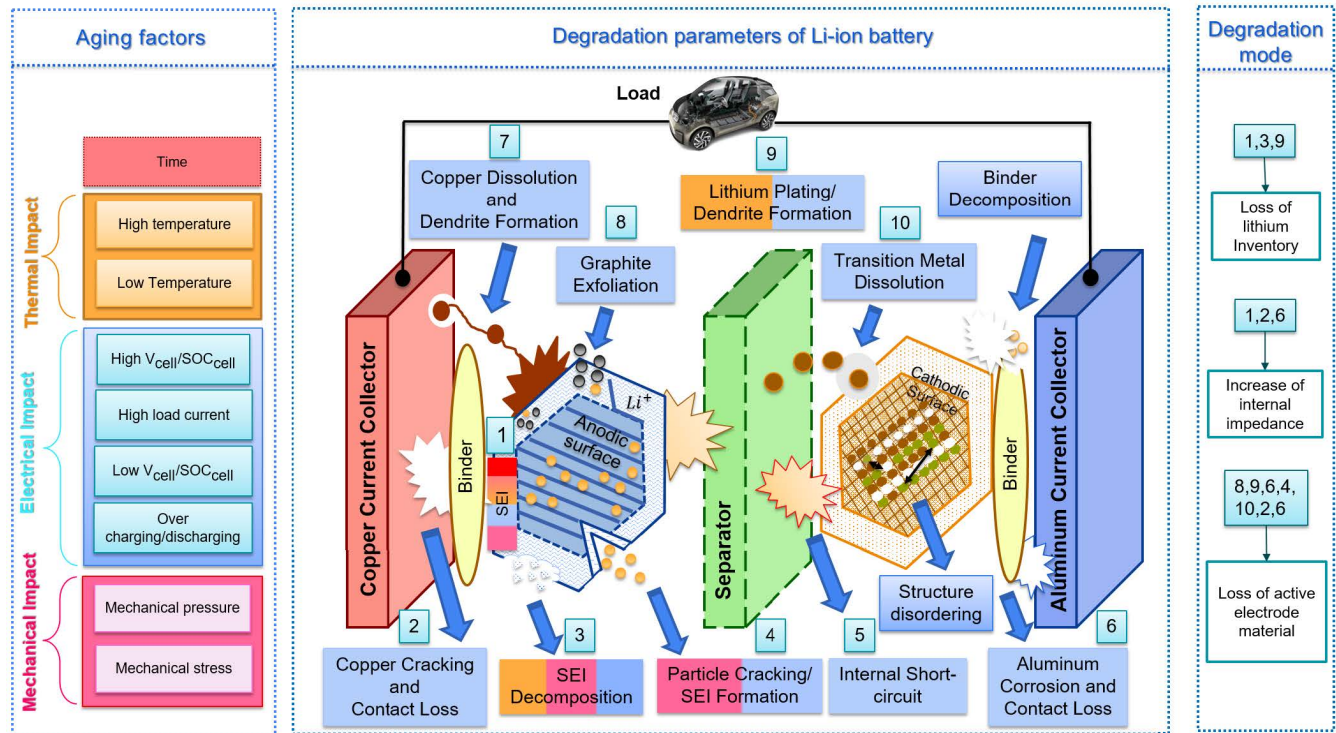


**FIGURE 8.** Representation of Li-ion battery aging factors and their associated degradation effects, modified version from [75].

ionic conductivity. An increase in electrolyte viscosity will also cause an increase in electrolyte density, which in turn increases the resistance of the electrolyte, which leads to a decrease in the ionic conductivity, ultimately decreasing the battery SOC. Secondly, as the viscosity of the electrolyte increases with a decrease in temperature, the charge transfer resistance will also increase. As a result, the kinetics of a battery will be greatly affected, as well as the flow of Li-ions within its electrodes, which reduces its performance. Lastly, the cold conditions will cause anodes to polarize, which will cause their potential to approach lithium metal, further delaying the intercalation of lithium into the anodes during charging. The aggregated Li-ions are then deposited on the electrode surface, reducing the battery capacity. Additionally, crystalline dendrites formed by lithium plating are capable of causing internal short circuits due to their ability to penetrate the separators [77].

Several recent studies have examined how low temperatures affect battery dynamics, particularly subzero temperatures [78], [79], [80], [81], [82], [83], [84]. The authors of [79], for instance, proposed a method for controlling the temperature of Li-ion batteries that leverages their increased internal resistance at subzero temperatures to increase the battery temperature until maximum power is achieved. Furthermore, the authors of [82] utilized a high-frequency sine-wave heater using resonant low-current converters to self-heat automotive battery packs in subzero temperatures without the need for an external heater. An additional study presented in [84] investigated both scenarios of the internal

and external heating of the battery (by drawing current from the battery, a convection heater is powered and by employing Joule heating, the cell is heated from inside).

## 2) HIGH TEMPERATURE EFFECT

High-temperature effects on Li-ion batteries are more complex than low-temperature effects. However, it is difficult to understand how to minimize the effect of the temperature increase during battery operation. The battery is heated by a number of processes, including chemical reactions and charge transfer between the electrode-electrolyte interface. Figure 9 shows all possible sources of heat generation and their corresponding chemical effects. As illustrated in Figure 9, many of these sources are related to irreversible processes, which are exothermic reactions. During the batteries are being charged or discharged, the exothermic heat generated by chemical reactions inside Li-ion batteries will affect battery chemical components, such as decreased lithium inventory due to SEI layer growth, metal dissolution, and electrolyte decomposition. As a result of the degradation of these chemical components, particularly the decrease in lithium concentration, battery capacity will decrease. In general, the heat generated by batteries affects their aging, as well as maybe causing thermal runaway issues.

The increase in temperature is considered to be one of the main causes of battery aging, and it might also potentially damage the battery. Battery aging is defined by the deterioration of the battery performance, as well as reducing the battery lifespan. The aging process of a battery accelerates as

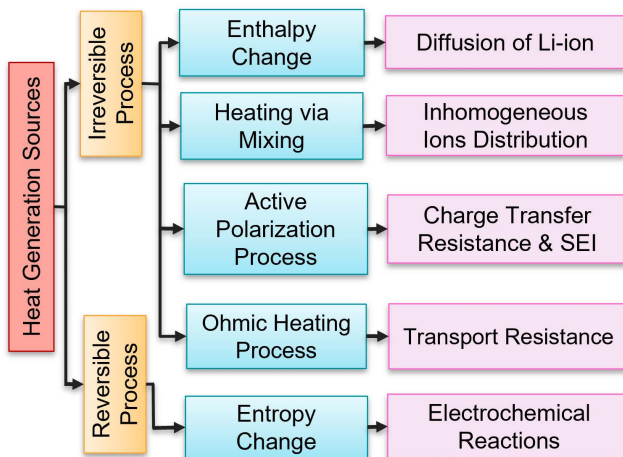


**FIGURE 9.** Classification of heat generation sources from Li-ion batteries and their impact on the chemical components of the batteries.

its temperature rises above a certain level, defined as thermal aging. At high temperatures, the thickness of the SEI layer increases, resulting in capacity fading. The SEI layer typically has a thickness in the micrometer range. However, it continues to thicken with battery aging, reducing the electroactive surface area of the negative electrode [85].

Thermal runaway occurs when the battery's internal temperature increases. This could be due to a battery failure, impact, or abuse. The chemical reactions occurring within the battery during operation are often exothermic in nature. These exothermic reactions are considered responsible for the increased battery temperature. This will lead to the exothermic decomposition of the battery material. Typically, Li-ion batteries generate a considerable amount of heat, which is challenging to handle. Therefore many researchers are investigating methods for controlling the generation of heat. For example, in [86], a multistage AC heating scheme is proposed to reduce the heating time without causing damage to the Li-plating.

#### B. ELECTRICAL ABUSE

Electrical abuse happens when a battery is overcharged, over-discharged, or short-circuited, leading to a series of chemical reactions resulting in significant performance issues and safety concerns.

##### 1) OVERCHARGING/OVER-DISCHARGING EFFECTS

An Overcharging/over-discharging of a battery can speed up its degradation and cause an early EOL. Increased battery degradation is due to undesirable side reactions within the battery, resulting in cyclable Li-ions and active material loss [87]. Particularly, the excessive delithiation (draw all active Li-ions) of the anode causes decomposition of SEI when the anode is over-discharged [87]. On the one hand, when batteries are over-discharged, their capacity decreases faster since the amount of degradation depends on the depth

of discharge (DOD). Furthermore, the over-deintercalation of Li causes an irreversible phase change and the collapse of the cathode, which results in the release of gas and the generation of heat. On the other hand, when batteries are overcharged, the anode becomes over-lithiated and the cathode becomes over-delithiated (no active Li-ions). In over-delithiated cathodes, structural changes are irreversible which causes an increase in resistance and degradation of the electrolyte when they are overcharged [31]. An overcharged battery may generate significant heat due to side reactions at both electrodes [88].

#### 2) HIGH CURRENTS EFFECTS

High current has the same deterioration effects that result from overcharging and over-discharging. High currents generate more heat, consequently, speeding up the aging process. Furthermore, changing the current level significantly impacts the electrochemical parameters (SEI layer growth, electrode particle cracking, loss of electric contact, and lithium plating), leading to performance degradation. Due to the Li-ion battery's organic electrolyte, its relatively low heat capacity makes it susceptible to temperature rises that are particularly rapid when current flows, as opposed to water-based batteries. In addition, fast-charging graphite anodes will result in metallic lithium-plating because graphite cannot accept Li-ions at high current rates [89].

#### C. MECHANICAL ABUSE

Mechanical impact or abuse of batteries could result from mechanical stress/strain or mechanical pressure. In principle, the battery volume expands if a certain threshold of strain is exceeded. These types of aging factors are responsible for SEI layer growth and cracks in electrode particles.

##### 1) MECHANICAL PRESSURE EFFECT

Mechanical pressure results from a manufacturing defect or an externally applied pressure. In such a case, the penetration or crash of the battery will cause the battery to explode [90]. It is recommended to use rigid battery casings in some applications (e.g., EVs) to prevent pressure from external forces.

##### 2) MECHANICAL STRESS AND STRAIN EFFECTS

Mechanical stress and strain are more important than mechanical pressure since they result from chemical reactions inside the battery. There are several sources of mechanical stress and strain in batteries, including the expansion of gas, the expansion of electrode materials during operation [87], and external loading. It is worth noting that the cracking and fracturing of electrode particles cause an internal short circuit near the separator [74], which generates high stresses. In the case of over-stressing an electrode, cracking or fracturing may occur, resulting in material failure. Thus, the battery's performance is significantly degraded and capacity fades [87].

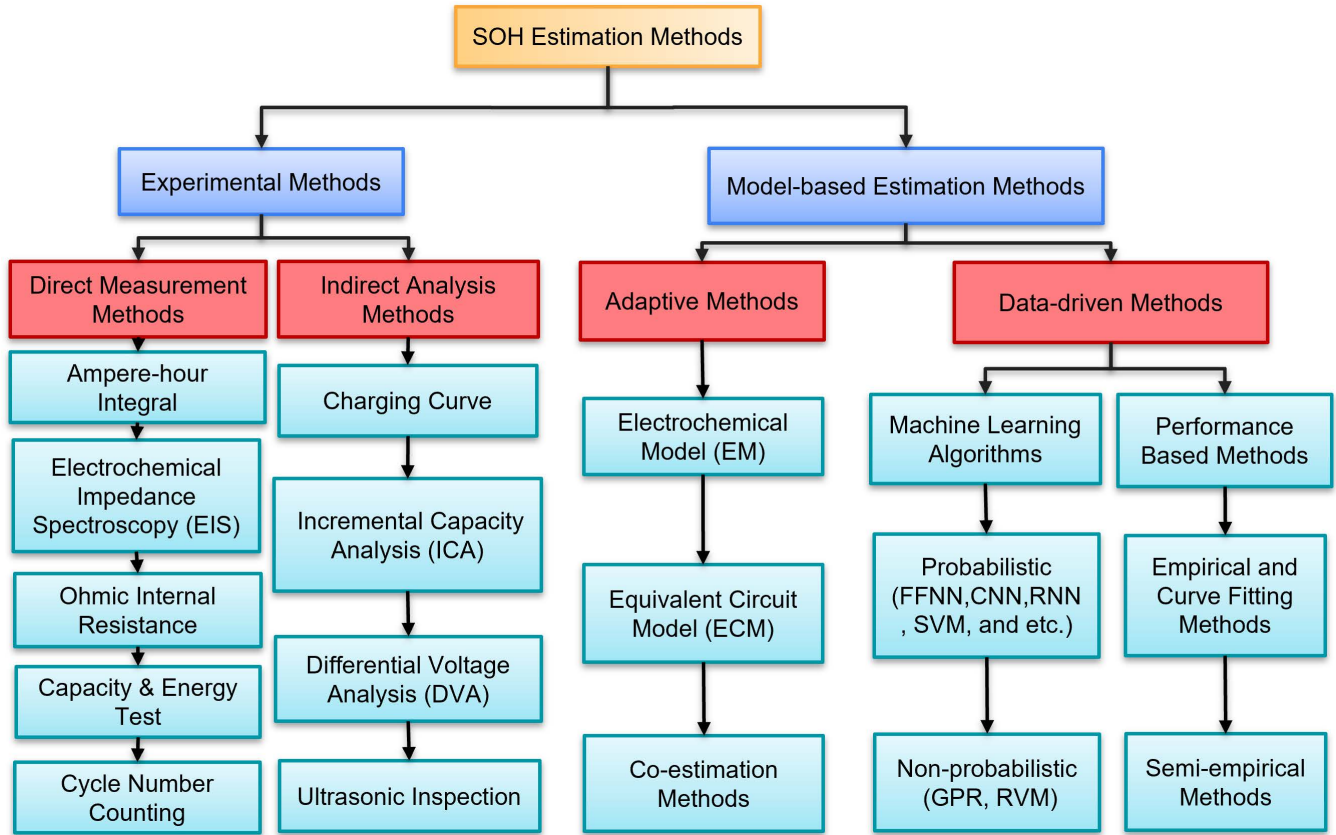


**FIGURE 10.** An overview of the various methods for estimating the SOH of Li-ion batteries.

## VI. LI-ION BATTERY SOH ESTIMATION METHODS

Complex chemical reactions trigger irreversible changes to the battery's characteristics during its operation. The SOH indicates the battery aging stage, which measures the actual age of the battery during its operational lifetime [4]. A battery's SOH can be defined in two ways: either according to the *capacity loss* or according to the *power fade*. The capacity loss of a battery is due to the increase in internal resistance and decrease in lithium inventory caused by chemical reactions within the battery over time. When the capacity of the battery falls to 80% of its original value, it indicates the battery has reached its EOL, and will then enter its second life.<sup>1</sup> According to this definition, the SoH is given by [91]:

$$SOH = 1 - \frac{C_i - C_b}{0.2 C_i}, \quad 0.8 C_i \leq C_b \leq C_i \quad (6)$$

where  $C_i$  is the battery capacity before usage (capacity at the BOL) and  $C_b$  is the capacity of the battery with any value before its EOL. The SOH lies within the range  $0 \rightarrow 1$ , in which zero means that the battery reached its EOL ( $C_b = 0.8 C_i$ ) and needs to be replaced. According to the

<sup>1</sup>In the second life, the battery still has significant energy storage capacity, but it does not provide sufficient power to drive an EV. However, it can be used for other applications such as stationary energy storage, which is used by grid operators, hospitals, etc.

second definition of SOH, power fade refers to the reduced amount of power that can be delivered to a load when the internal resistance of the battery increases. In this case, the battery is considered to be at its EOL when its internal resistance is doubled. By considering the battery's internal resistance, the SOH can be expressed as follow [91]:

$$SOH = 1 - \frac{R_b - R_i}{R_i}, \quad R_i \leq R_b \leq 2R_i \quad (7)$$

where  $R_i$  is the battery initial resistance and  $R_b$  is the resistance of the battery at any age. When  $R_b = 2 R_i$ , the SOH drops to zero and the battery needs to be replaced (reached its EOL).

Several methods have been developed over the years for estimating the SOH of Li-ion batteries. In general, there are two main categories of SOH estimation methods: 1) *experimental-based*, and 2) *model-based*. Across all of these methods, we are aiming to achieve an accurate estimation of the battery age by assessing the battery's SOH with less computational complexity. A summary of most of the available methods for estimating SOH is shown in Figure 10. The experimental methods are based on measuring the battery parameters (lithium concentration, capacity, internal resistance, voltage, current, etc) and storing them to analyze how these parameters are changing during the

**TABLE 3.** Comparison of battery SOH estimation methods.

	Method	Advantages	Disadvantages	Improvement suggestions
Experimental methods	Direct measurement methods [92–94]	<ul style="list-style-type: none"> <li>• Easy to implement</li> <li>• Combine easily with model-based</li> <li>• EIS is useful for studying aging processes</li> <li>• High accuracy in laboratory climate</li> </ul>	<ul style="list-style-type: none"> <li>• Online measurements are difficult</li> <li>• Require high performance equipment</li> <li>• Destructive methods can permanently damage the battery</li> <li>• Unsuitable for real-time applications</li> </ul>	<ul style="list-style-type: none"> <li>• Implement EIS using pseudo-random sequence instead of sinusoidal signal</li> <li>• Identify offline strategies for maintenance and diagnosis</li> <li>• Combined with a suitable battery model</li> </ul>
	Indirect analysis methods [95–97]	<ul style="list-style-type: none"> <li>• High accuracy in lab environment</li> <li>• Online battery aging using ultrasonic measurements &amp; ICA/DVA</li> <li>• Estimate battery SOH using external characteristics</li> </ul>	<ul style="list-style-type: none"> <li>• Require constant current for ICA/DVA charging curve methods</li> <li>• Unsuitable for all battery formations</li> <li>• Temperature changes affect accuracy</li> <li>• Online application is difficult</li> </ul>	<ul style="list-style-type: none"> <li>• Consider the temperature effect</li> <li>• Incorporating with ML algorithms</li> <li>• Online methods to obtain DVA&amp;ICA curves which require less computation complexity</li> </ul>
Model-based estimation methods	Adaptive filtering methods [24, 96, 98–100]	<ul style="list-style-type: none"> <li>• Provide trade-off between estimation accuracy and computational complexity</li> <li>• Different battery chemistries can be used for online battery aging</li> </ul>	<ul style="list-style-type: none"> <li>• Model accuracy depends on parameter identification</li> <li>• Need high-performance controllers</li> <li>• Require massive experimentation to develop an algorithm</li> </ul>	<ul style="list-style-type: none"> <li>• Developing multi-model fusion can enhance model applicability</li> <li>• Considering more physical parameters can improve ECM</li> </ul>
	Empirical& data fitting models [101–104]	<ul style="list-style-type: none"> <li>• Accurate to estimate battery SOH</li> <li>• Reduce number of required pre-tests</li> </ul>	<ul style="list-style-type: none"> <li>• Highly depend on quality of information</li> <li>• Algorithm efficiency&amp;portability are highly demanded</li> </ul>	<ul style="list-style-type: none"> <li>• Adaptive filtering methods can be combined to enhance the accuracy &amp; robustness of on-board battery SOH estimation</li> </ul>
	ML models [105–113]	<ul style="list-style-type: none"> <li>• High SOH estimation accuracy</li> <li>• Not required physical/chemical information</li> <li>• Suitable for on-board estimation</li> </ul>	<ul style="list-style-type: none"> <li>• Estimation accuracy is sensitive to dataset quality</li> <li>• Computational effort is high</li> </ul>	<ul style="list-style-type: none"> <li>• Gathering high quality and sufficient quantity of battery information can achieve through using a big data&amp; cloud technology</li> </ul>

battery life. These estimation methods are divided into two subcategories: *direct* and *indirect methods*. Even though the direct methods are simple and more efficient, they can only be applied to offline battery health estimation and are limited to small batteries (i.e., large batteries such as those in EVs require complex operations). Consequently, these methods are generally limited to laboratories for assessing various battery aging parameters. For indirect methods, analyzing and processing the measured battery data is necessary. However, these methods are not generalized to all EVs since the measured data depends on a specific battery form (cylindrical, prismatic, or Pouch). Thus, it is important to validate these methods under different battery forms. In recent literature, a variety of indirect methods have been proposed to estimate the battery's SOH, for example, the work in [95] uses  $V_{oc}$ (SOC) battery characteristic to estimate the SOH online. In [96], the authors developed a double exponential degradation model based on the strong correlation between the SOH, and the online discharging voltage and time measurements (which are used as health indicators). Then, they used an unscented particle filter to adjust the model parameters in real time in order to estimate the SOH from those health indicators. A study presented in [97] estimated the battery SOH using incremental capacity analysis (ICA) for battery packs with cell-level battery tests.

On the other hand, model-based methods, are further divided into two subcategories, namely *adaptive filtering*, and *data-driven estimation* methods. Adaptive filtering methods are introduced as a solution to the challenges faced by indirect measurement methods. In other words, these filtering methods can be applied to various battery chemistries as

they reduce the dependence of the SOH estimation on the measured battery parameters. Despite having these methods with a high degree of accuracy, they are burdened by the required high computational complexity. These methods are based on identifying battery parameters (i.e., only the external parameters such as voltage, current, and temperature) using various optimization algorithms [114]. Then, they use these parameters to estimate the SOC and SOH of a battery using an adaptive filter, such as the Kalman filter family [24], [98] and particle filter [96], [99]. For example, the ECM of the battery is used in [115] where SOH is treated as part of the model state and estimated using a Kalman filter. In another study presented in [24], SOH was calculated using the Coulomb counting method for an ECM battery model of second order. Then, an extended Kalman filter and online battery parameter identifications are used to estimate the SOH. In [100], a third-order ECM is used to model the battery where the internal resistance of the battery is used as part of the state. Then interactive multiple models are used to estimate SOH. To estimate the voltage response, the authors of [116] proposed a scheme that co-estimates SOC and SOH through fractional-order equivalent circuits. A hybrid genetic algorithm/particle swarm optimization (PSO) method was used to parameterize the fractional circuit model. Although this scheme improves SOH estimation accuracy, it is moderately complex. Consequently, it is crucial to strike a balance between the accuracy of the SOH estimation and the complexity of the model. Because of the variability in operating conditions, electrochemical and ECM-based models may not remain accurate. Generally, estimating the SOH accurately remains a challenge.

This paper focuses on data-driven methods for estimating the SOH, including *empirical models* and *machine learning models* such as support vector machine (SVM) [38], [73], Gaussian process regression (GPR) [40], [117], logistic regression [118], artificial neural networks (ANN) [69], [70], Markov chains [71], [108], recurrent neural network (RNN) [110], k-nearest neighbors (KNN) [111], and random forest regression (RFR) [112]. The following section presents detailed information about data-driven methods. Additionally, in Table 3, we compare a variety of methods for SOH estimation including some suggestions for improvement. For more information, there are several other review papers have discussed the estimation of the SOH [25], [26], [119], [120].

#### A. DATA-DRIVEN METHODS FOR BATTERY SOH ESTIMATION

Data-driven methods have gained increasing attention for estimating battery SOH because they do not require an understanding of implicit changes in battery chemical parameters or working principles. Consequently, these methods provide an alternative to traditional SOH estimation methods which normally require an extensive measurement of battery parameters during its operation to provide an accurate battery model and health estimation. However, to achieve a high SOH estimation accuracy using data-driven methods, a large amount of battery parameter features needs to be collected, which remains a challenge and requires high computational efforts.

##### 1) EMPIRICAL AND DATA FITTING ALGORITHMS

Empirical and data fitting algorithms use available measurements of battery features to give an estimate of Li-ion battery age. The most common fitting methods are polynomial, exponential, and power law. One of the benefits of using empirical methods is that they require less computation time due to their simplicity. Most reviews of the literature on the estimation of battery health considered SOC,  $\Delta$ SOC, the voltage at charge and discharge, temperature change, and DOD as the most significant features that characterize the age of the battery. In general, empirical models are built by analyzing laboratory data and then applying a fitting method to estimate the capacity loss (an indirect measure of the SOH). This means that the higher the quality of the data, the more accurate the battery capacity estimation will be.

Different models have been developed to estimate the *capacity loss* associated with various aging factors [101], [102], [103], [121]. The capacity loss model, for instance, proposed in [104] is based on the results from a large matrix of battery cycle tests that include three main battery features: the DOD in range (90→10%), temperature to be changed between (-30→60 °C), and discharge C-rate which is varying in the range 0.5C → 10C with the 1C rate corresponding to 2A. Along with the empirical capacity models, an empirical method is proposed in [102] to estimate the battery capacity by using a DC charger and equipment to measure the voltage and current flowing from the charger to the battery. In this study, the method is used to gain a unique insight

into how vehicle-to-grid can affect batteries performing an energy-intensive form of grid service. They compared the empirical model results with actual measurements of capacity, which estimated a similar degradation but attributed 2/3 of the capacity loss to aging and 1/3 to cycling. In [103] a hybrid model based on a feed-forward empirical model and a feed-back data-driven model is developed to deal with the issue of mismatches in battery parameters and the uncertainty of online capacity estimations. A recursive least squares algorithm with a forgetting factor is applied to calculate the difference between the estimates of capacity made by an empirical method and a data-driven method; the parameter feed-back correction algorithm is used to dynamically modify and update the parameters of the empirical models. Then, the capacity fusion correction algorithm combines the predictions from the modified empirical model with the data-driven estimates in order to achieve the fusion capacity. According to this hybrid method, the fusion capacity can be estimated; however, it needs several feed-back corrections to achieve high estimation accuracy of capacity, which could be a reflection of the SOH.

#### 2) MACHINE LEARNING ALGORITHMS

The use of ML algorithms automates the process of building analytical models from data [31]. This approach is based on the notion that the system can learn from historical data or experiences, and make decisions or estimates without relying on human intervention. Several ANN algorithms are developed to estimate the SOH, including feed-forward neural network (FFNN), radial basis function (RBF) neural network, RNN, hamming neural networks (HNN), etc. An advantage of using ANNs for estimating SOH is their high accuracy and computing speed (i.e. no knowledge of the battery's physical characteristics is required). However, obtaining a comprehensive dataset is challenging and requires high computational efforts. Figure 11 illustrates the framework of using ML models, ANNs, to estimate the SOH for EVs. In the first stage, sensors such as voltage, current, and temperature collect data from the EV's battery pack (i.e., from each battery module, see Figure 11). In the next stage, the BMS processes the sensed data by filtering irrelevant data and taking into account only those features that have a significant influence on the aging of the battery (capacity loss/power fade). Then applies the processed data as inputs to stage 3 to train an ANN model (details are provided in Section VIII). In the final stage, after the ANN model is trained, the model will be implemented into the BMS for estimating the SOH.

Various recent studies have utilized ML algorithms to estimate the SOH using a variety of datasets such as [105], [108], [109], [122], [123], [124], [125], [126], [127], [128], [129], [130]. Table 4 compares some of these models and summarizes their results (details about these ML models will be discussed in Section VII). In this table, the comparison of SOH estimation errors is provided based on root/mean square error (R/MSE) or mean absolute (percentage) error (MA(P)E). For example, the work in [123], [109], [105], [108], [125],

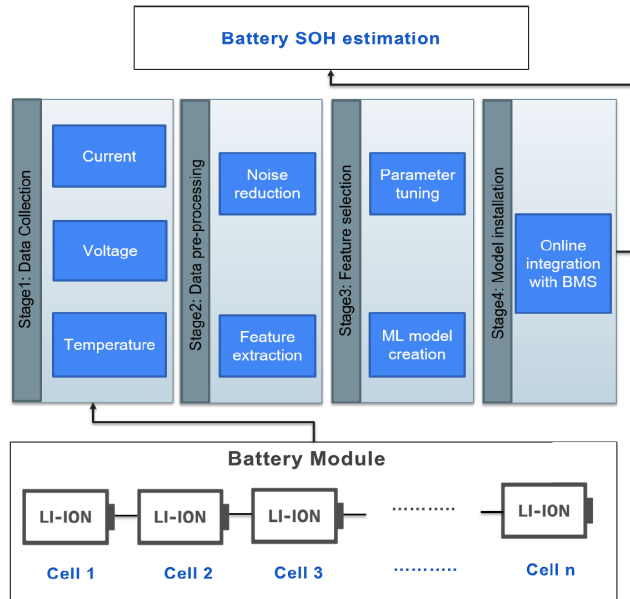


**FIGURE 11.** A generic workflow of developing an ML model for estimating the battery SOH.

and [126] presented various ML models including relevance vector machine (RVM) and LSTM with PSO, prior knowledge-based neural network with Markov chain (MC-PKNN), convolutional neural network (CNN) and Bi-directional LSTM, FFNN and RNN, support vector regression (SVR), and SVM with RBF, respectively to estimate the SOH. All of these aforementioned models were developed using battery degradation data collected by NASA [131], allowing a fair comparison of the SOH estimation error among them. Based on these comparisons, it can be observed that hybrid models such as bi-directional LSTM, PA-LSTM, MC-PKNN, or SVM with RBF achieve better results compared to the traditional single models. Additionally, MC-PKNN and SVM with RBF have the lowest estimation errors, which suggests that more investigation will need to be conducted on those models under different test conditions and on different datasets in the future. Furthermore, combining several other ML models may result in better SOH estimation.

## VII. LI-ION BATTERY REMAINING USEFUL LIFE PREDICTION METHODS

RUL has been defined in various ways by different researchers in this field. Generally, once the battery is put into service, it begins to age until it reaches its EOL and needs to be replaced. Battery RUL is used to predict the remaining time for a battery before it reaches its EOL, however, there is no universally accepted definition of battery EOL. Specifically, the RUL can be defined in two different ways: either according to *the calendar life* or according to *the cycling life*. On the basis of the calendar life definition, the RUL is predicted as a function of time (i.e., months or years). Nevertheless, the battery may reach its EOL before the calendar's prediction. Alternatively, on the basis of the

cycling life definition, the RUL is determined by predicting the number of cycles the battery can complete before it reaches its EOL. However, in some instances when the battery is not cycled in a normal way, it can be difficult or even impossible to determine a precise cycling number. In addition, EVs with battery packs containing hundreds or thousands of batteries may perform differently from battery to battery, as well as the number of cycles may vary from one battery to another.

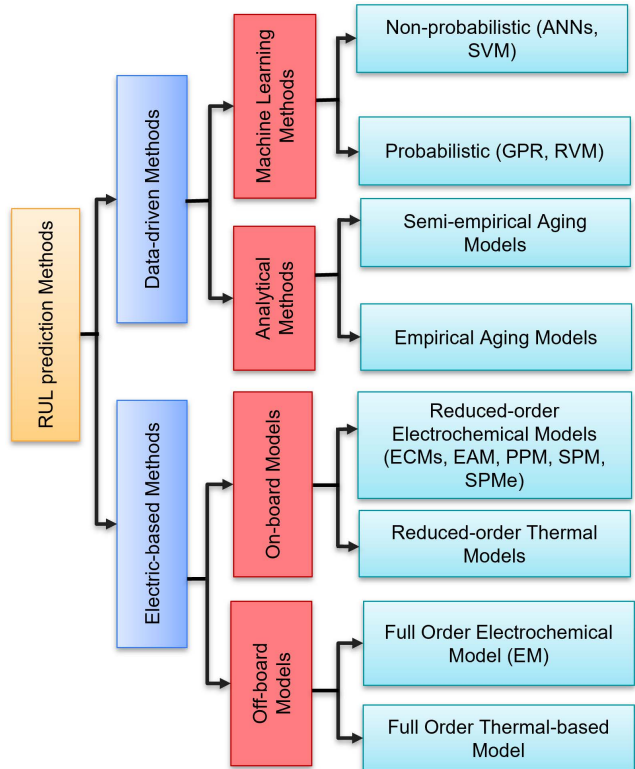


**FIGURE 12.** Classification of the RUL prediction methods.

In contrast to SOH estimation which provides information about battery age at a certain time, RUL prediction makes use of SOH information to predict the residual life of the battery. The RUL prediction methods can be divided into two main categories: 1) *electric-based methods*, and 2) *data-driven methods*. RUL prediction using the electric-based methods can be performed either onboard (during battery operation) or off-board, depending on the complexity of the battery model being used (detail of electrical battery models is discussed in Section IV-A). Alternatively, data-driven methods can either be empirical or semi-empirical (SeMs), which calculate by fitting mathematical equations, or ML models based on battery degradation data. This classification of the RUL prediction methods is illustrated in Figure 12. In this paper, we present an overview of electric-based RUL prediction methods with a focus on data-driven methods. Table 5. presents a comparison of these prediction methods in terms of their strengths and weaknesses, along with suggestions for improving each method.

**TABLE 4.** Comparison of various ML models for estimating the SOH.

ML algorithm	Battery type	SOH Methodology	Temperature range	Dataset	Lowest error rate (at 25°C)
FFNN [122] classifier	Battery pack of 13 Lithium cells connected in series	In→ variation of (SOC, V, C, E and T) Out→ SOH (75%→100% with 5% step)	(20→60°C) with 5°C step	CALCE**	classification error of 0.6% for current profile 1, and 1.3% for current profile 2
FFNN [123] regressive	Li-ion battery 18650 with $C_{BOL} = 2$ Ah (NMC)	In→ multi-channel (V, I, and T) Out→ C in Ah (EOL at C= 1.4 Ah)	25°C	NASA*	RMSE→ 0.0298, and MAPE→ 1.73% with 40 neurons in the hidden layer
FFNN [124] with k-means	Pack of Li-ion 18650 cells with $C_{BOL} = 3.1$ Ah	n→ multi-channel (V, I, and T) Out→ C in Ah (during charging)	10, 25, 45, and 60°	UDDS <sup>+</sup>	RMSE→ 0.0677 (less than 2.18% error on average)
RNN(LSTM) [123]	Li-ion battery 18650 with $C_{BOL} = 2$ Ah (NMC)	In→ multi-channel (V, I, and T) Out→ C in Ah (EOL at C= 1.4 Ah)	25°C	NASA*	RMSE→ 0.0246, and MAPE→ 1.032%
Bi-directional LSTM [109]	Li-ion battery 18650 with $C_{BOL} = 2$ Ah (NMC)	In→ multi-channel (V, I, and T) Out→ C in Ah (EOL at C= 1.4 Ah)	25°C	NASA*	RMSE→ 0.01, and MAPE→ 0.0081 for battery#5 (forward/backward processing)
PA-LSTM [105]	Li-ion battery 18650 with $C_{BOL} = 2$ Ah (NMC)	In→ multi-channel (V, I, and T) Out→ C in Ah (EOL at C= 1.4 Ah)	25°C	NASA*	RMSE→ 0.006 for battery#5 based on PSO and Attenuation mechanism (PA)
RVM [105]	Li-ion battery 18650 with $C_{BOL} = 2$ Ah (NMC)	In→ multi-channel (V, I, and T) Out→ C in Ah (EOL at C= 1.4 Ah)	25°C	NASA*	RMSE→ 0.0141 for battery#5 (training on 70% of the raw data)
CNN [109]	Li-ion battery 18650 with $C_{BOL} = 2$ Ah (NMC)	In→ multi-channel (V, I, and T) Out→ C in Ah (EOL at C= 1.4 Ah)	25°C	NASA*	RMSE→ 0.0482, and MAPE→ 0.0514 for battery #5
MC-PKNN [108]	Li-ion battery 18650 (2Ah) (NMC) LiFePO4 battery	In→ $V_{avg}$ (charge/discharge), $t$ (charge), $\Delta V$ (at fixed time), $dSOC/dV$ (peak) Out→ C in Ah	25°C	NASA* Commercial battery****	MSE→ 0.2145% for battery #5 (NASA), and MSE→ 0.0076% for battery #1 (commercial battery data)
SVR [125]	Li-ion 18650 (NMC) 8 small Li-ion pouch cells (NCA)	In→e DT curve (dT/dt vs. V) & ICA curve (C vs. V) Out→ C in Ah	25°C NASA 40°C Oxford	NASA* Oxford***	RMSE→ 2.49%, MAE→ 4.9% (NASA) RMSE→ 1.08%, MAE→ 2.5% for battery #3 (Oxford), both for DT curve
SVM [126] with RBF	Li-ion battery 18650 with $C_{BOL} = 2$ Ah (NMC)	In→ all features (V, I, and T) Out→ C in Ah (EOL at C= 1.4 Ah)	25°C	NASA*	MSE(10 exp -4)→ 0.45, MAPE→ 0.59% for battery#3
ELM [127] Extreme Learning Machine	3 (LiNMC) batteries with $C_{BOL} = 2.6$ Ah	In→ variation in ohmic & polarized R ( $\Delta R$ ), Out→ C in Ah	25°C	UDDS <sup>+</sup> & NEDC <sup>++</sup>	RMSE→ 0.0109, MAE→ 1.72%, Max Error→ 2.22%
RF [128]	Pouch batteries (NMC) 17 with 20 Ah (type A) 6 with 31.5 Ah (type B)	In→e , Out→ C in Ah	25°C	charging (V-C) curves	RMSE→ 0.48 %, MAE→ 0.36%, and Max Error→ 2.22% for battery#3 (type A) RMSE→ 0.53% for battery#3 (type B)

NASA\* is a battery degradation dataset collected by NASA Ames Prognostics Center of Excellence (NAPCE) [131]

CALCE\*\* is a battery degradation dataset collected by Center for Advanced Life Cycle Engineering at the University of Maryland [132]

Oxford\*\*\* is a battery degradation dataset collected by a research group at the University of Oxford [133]

Commercial battery\*\*\*\* is a battery degradation data collected by Hefei Guoxuan High-Tech Power Energy Co., Ltd., China [134]

UDDS<sup>+</sup> stands for Urban Dynamometer Driving Schedule and represents dynamic driving profiles within a city collected by EPA in the USA

NEDC<sup>++</sup> stands for New European Driving Cycle and represents dynamic driving profiles for vehicles in Europe

#### A. ELECTRIC-BASED RUL PREDICTION METHODS

Several battery models have been developed to predict the RUL of Li-ion batteries based on the battery electrochemical parameters as discussed previously in Section IV. In this section, we review the methods of predicting battery RUL based on the complexity of the model, which can be classified into two categories: *off-board* and *on-board* predictions.

##### 1) OFF-BOARD ELECTRIC-BASED RUL PREDICTION METHODS

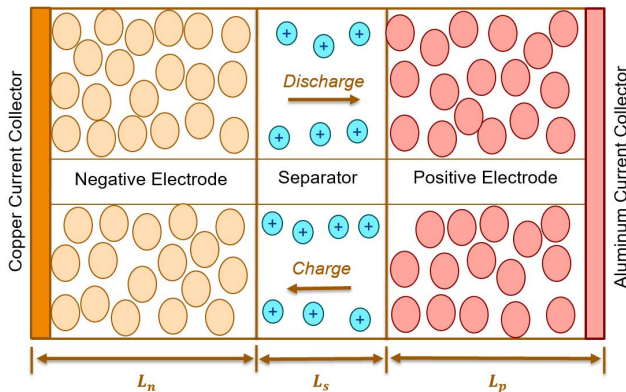
Figure 13 shows the P2D model for a Li-ion battery which has a separate structure for each part of the battery (negative electrode, positive electrode, and separator). The mass and charge conservation in these parts are expressed in a set of governing PDEs. These PDEs describe the diffusion, migration, and reaction kinetics inside the battery. The equations that describe the diffusion of Li-ions at the solid phase (positive and negative electrodes) and the transportation of Li-ions in the electrolyte phase can be found in [59].

The RUL of a battery is determined by the lithium concentration available for producing an electrical charge. However, solving the PDEs of the full-order P2D model is challenging. Experimental evidence confirms that the full-order P2D is the most convenient way to simulate the actual electrochemical dynamics of Li-ion batteries [135]. In practice, however, using this method to predict battery RUL for applications containing hundreds to thousands of batteries, such as the battery pack for EVs, becomes problematic, since the simulation time could take months [135]. A set of optimization techniques is proposed for estimating the unknown parameters of PDEs in order to enable the use of the full P2D model.

Unlike the on-board parameter identification methods (discussed in the following section), off-board methods do not need to find optimal parameters during battery operation. Therefore, they can deal with the full-order P2D model. Using voltage and current measurements for a recent time period, they determine the parameters that are likely unknown. The term “likely unknown” refers to variables identified using

**TABLE 5.** Comparison of Li-ion battery RUL prediction methods.

	Method	Advantages	Disadvantages	Enhancing ways
Electric-based prediction techniques	Offline prediction techniques	<ul style="list-style-type: none"> <li>Provide all information on battery dynamic characteristics</li> <li>High estimation performance of battery health</li> </ul>	<ul style="list-style-type: none"> <li>More complex to implement</li> <li>Unknown parameters need to identify</li> <li>Estimation accuracy sensitive to parameter identification accuracy</li> </ul>	<ul style="list-style-type: none"> <li>Use more accurate parameter identification approaches</li> <li>With high-performance processors, online applications may be possible</li> </ul>
	Online prediction techniques (ROEMs / ECMs)	<ul style="list-style-type: none"> <li>Easy to implement with the BMS</li> <li>Reduce the complexity of EMs</li> <li>Acceptable accuracy of battery health estimation</li> </ul>	<ul style="list-style-type: none"> <li>Assumptions to simplify EM cause loss of important information</li> <li>Complexity of ECMS <math>\propto</math> Number of RC-networks</li> <li>Models as EAM not practical validate</li> </ul>	<ul style="list-style-type: none"> <li>Consider the degradation factors such as high current effects, and overcharge/over-discharge</li> <li>Incorporating with ML algorithms to improve the system complexity</li> </ul>
Analytical prediction techniques	Semi-empirical aging model	<ul style="list-style-type: none"> <li>BMS can easily monitor battery life for online applications</li> <li>Parameters extraction is easy</li> <li>Model construction is simple</li> <li>Fast in estimating battery SOH</li> <li>Fewer computation efforts</li> </ul>	<ul style="list-style-type: none"> <li>Developed models are not universal</li> <li>Require specific operating conditions for each battery type</li> <li>Require more laboratory tests</li> <li>Take a long time and expensive</li> <li>Aging tests are difficult in laboratory</li> </ul>	<ul style="list-style-type: none"> <li>Test various battery formations with various characteristics to find a relation between them</li> </ul>
	Empirical aging model	<ul style="list-style-type: none"> <li>Actual measurements update estimation errors</li> <li>Modeling aging process requires little aging data</li> </ul>	<ul style="list-style-type: none"> <li>Online applications are more difficult</li> <li>Require high computational efforts</li> </ul>	<ul style="list-style-type: none"> <li>Improve the mathematical representation of the model to achieve better computational efforts</li> </ul>
Machine learning Non-probabilistic	ANN	<ul style="list-style-type: none"> <li>Recurrent link makes RNNs an excellent long-term forecasting</li> <li>Possess an in-depth understanding of non-linearities</li> <li>Optimal prediction accuracy</li> </ul>	<ul style="list-style-type: none"> <li>Cannot deal with battery nonlinearity</li> <li>Incapable to handle uncertainty</li> <li>Possibility to cause over-fitting issues</li> <li>Performance of the model is greatly influenced by the training process</li> </ul>	<ul style="list-style-type: none"> <li>Collect more battery features to provide more information on battery dynamics</li> <li>Combining different ANNs together to improve battery SOH estimation</li> </ul>
	SVM	<ul style="list-style-type: none"> <li>Accurate prediction</li> <li>Robustness in the face of outliers</li> <li>Analyzes without parametric variables</li> <li>Prediction time is short</li> </ul>	<ul style="list-style-type: none"> <li>Difficult to handle nonlinearities in battery parameters</li> <li>Need to determine hyper-parameters by cross-validation</li> <li>Computational cost is high</li> </ul>	<ul style="list-style-type: none"> <li>Using a hybrid model instead of a single model will improve the system performance for handling the non-linearity such as GPR model with SVM</li> </ul>
Machine learning probabilistic	GPR	<ul style="list-style-type: none"> <li>Support high flexibility</li> <li>Provide co-variance to generate levels of uncertainty</li> </ul>	<ul style="list-style-type: none"> <li>Very expensive to compute</li> <li>Kernel functions have a high impact on performance</li> </ul>	<ul style="list-style-type: none"> <li>Enhance the quality and quantity of the dataset to improve the model robustness</li> <li>Select model parameters carefully to achieve the best possible results</li> </ul>
	RVM	<ul style="list-style-type: none"> <li>Accurate prediction</li> <li>Realize a high degree of sparsity</li> <li>Results are non-parametric</li> <li>Easily to create PDF</li> </ul>	<ul style="list-style-type: none"> <li>Local optimization issues easy occur</li> <li>Consume large time in training process</li> <li>Potential to cause over-fitting issues</li> <li>Modeling requires plenty of data</li> </ul>	<ul style="list-style-type: none"> <li>Gather high-quality datasets &amp; accurately sampling&amp;pre-processing them to avoid over-fitting</li> </ul>

**FIGURE 13.** P2D electrochemical model representation of Li-ion battery.

data in order to minimize the differences between measurements and predictions derived from this model. By using Jacobian and random search methods, for instance, this

difference can essentially be minimized. Nevertheless, these methods can get stuck in local optima, and thus cannot create an accurate parameter identification. Note that inaccurate identification of these parameters will adversely affect the accuracy of the prediction of the RUL. Thus, P2D becomes a more complicated model without gaining any benefit in terms of predicting the RUL. This is why the P2D model is commonly used on a laboratory scale since it yields highly accurate results when its parameters are identified correctly.

The authors of [136] used gradient-based, then local least-squares fitting in conjunction with the uncertainty quantification procedure to estimate parameter changes due to battery aging and to calculate confidence intervals for the parameter estimates. Lenze et al. [137] proposed a parameter identification approach for a full-order electrochemical model whose parameters were manually adjusted. Using a partially random-based optimization approach, Chun and Han [138] demonstrated how to estimate the parameters for the P2D model using a cascaded improved harmony search.

According to Laue et al. [139], a three-stage process is proposed which includes the use of quasi-static 3-electrode measurements of EIS, the open-circuit potential, and C-rate tests. According to their study, open-circuit potential testing and C-rate tests are not sufficient to parameterize the electrochemical model, which makes highly dynamic tests essential to resolve the inconsistency between diffusive and electric processes.

## 2) ON-BOARD ELECTRIC-BASED RUL PREDICTION METHODS

To deal with the complexity that arises from the full-order electrochemical (i.e., P2D) model, a set of reduced-order versions is developed for use in real time. Basically, the reduced P2D model simplifies the solution of diffusion PDEs in the solid phase. By applying volume averaging, the full-order P2D model can be simplified by reducing the coupled PDEs to a set of uncoupled ordinary differential equations (ODEs), and a set of analytical expressions. These reduced order models are referred to as ROEMs (outlined in Section IV-A). In obtaining the ROEMs, no physical insight is lost — all variables retain their physical significance. Additionally, these ODEs are easy to integrate and can be applied to on-board RUL prediction. In order to use the ROEMs to predict the RUL, unknown parameters must also be determined, such as lithium concentration on the electrodes, lithium concentration of the electrolyte, the resistance of the SEI layer, and solid/electrolyte fractions. Therefore, online parameter identification techniques are developed, such as improved recursive least squares [140], and Kalmen filters [141]. Once the battery parameters are identified, the RUL of the battery can be predicted using the ODEs.

Allam et al. [4] proposed an adaptive interconnected observer using the enhanced SPM that considers battery degradation parameters and their dependence on temperature change. This interconnected observer determines on-board the value of unknown battery parameters such as Li-ions concentration in the solid phase, battery capacity, diffusivity of the anode, and ionic conductivity at the SEI layer. The experimental results of this approach prove that the prediction error is around 1% for a fresh battery whereas 2% for an aged one. Additionally, capacity prediction remains robust to measurement errors and sensitivity bias. A major limitation is, however, that this method can only be applied to new vehicles since it requires overhauling the BMS. The authors of [142] developed an SPM model based on battery degradation factors that detects the capacity fade and two key degradation mechanisms. Specifically, at the anode electrode, the SEI layer growth is determined based on the lithium loss that causes chemical battery parameters degradation. While, at the cathode electrode, the volume change in active material due to dissolution, as well as the corresponding changes in the transport properties were also determined. This approach is successful in predicting the *remaining cycle number* of batteries based on *capacity fade* and *voltage profile change*

considering the lithium concentration loss as well as the volume fraction changes. According to their experimental results, the predicted capacity matches the measured value within a 1% margin. However, the model parameters are calculated empirically for each batch, and the model is not able to predict fluctuating current profiles.

ECM models simulate electrochemical parameters as electrical components, which are considered to be a simplified version of a full-order electrochemical model. To accurately predict RUL on-board, ECMS need to identify the circuit components that reflect actual changes in battery chemical parameters. Due to the accuracy of ECMS in predicting the RUL depending on the accuracy of identifying circuit parameters, a wide range of methods have been developed to accurately identify these parameters. For instance, Jussi et al. [143] proposed a novel fitting algorithm to determine the parameters of ECM based on the shape of the battery's internal impedance from the Nyquist plot. The authors of this paper used pseudo-random sequence (PRS) instead of the traditional way of measuring battery internal impedance such as sinusoidal signal, resulting in a shorter measurement time, maximum performance, and a decrease in complexity. The experimental results showed that their approach can predict the battery voltage accurately with RMSE 3.7% at 25°C and increased to 8.8% at 45°C when the battery SOC was adjusted at 90%. Another fractional-order circuit model is proposed by the authors of [144] where the EIS is first estimated using real-time voltage and current measurements. Then a regression model based on EIS was obtained and used in the framework of a particle filter to predict the RUL. A second-order ECM, as well as a thermal model of the battery, were used in [145], which determines first the core temperature and the capacity of the battery. Then the parameters of the aging model are identified online to predict the RUL. By using a stochastic model [146], [147], [148], [149], [150], the battery degradation is modeled as a random process with random drift. Then the drift in the degradation model parameters is estimated using different filtering methods.

## B. DATA-DRIVEN BASED RUL PREDICTION METHODS

### 1) DATA FITTING USING ANALYTICAL MODELS

Analytical models utilize mathematical equations that correlate a battery's aging status with its *calendar life* or *cycle number*. In the literature, there are two types of analytical models that have been developed: a) SeM with data fitting, and b) empirical model with data filtering. The SeM takes the form of an open-loop method, in which a vast amount of aging data are analyzed to determine the model parameters and the battery age (e.g., SOH or RUL). However, once the model is constructed, the developed model cannot change these battery parameters (no feedback). The latter takes the form of a closed-loop method, meaning that as new information or data becomes available, the model parameters are adjusted accordingly.

### a: SEMI-EMPIRICAL MODELS WITH DATA FITTING

The SeMs are derived using the mathematical expression of battery performance that depends on the direct relationship between battery aging factors and battery capacity. In other words, the SeM models rely on the battery characteristics that are often measured over the battery's lifetime. These models are built using a variety of interpolation and fitting information obtained from a set of experiments. For an accurate estimation of the battery life as well as for a prediction of how long the battery will last, a comprehensive aging analysis taking into account various operating conditions must be performed. However, assessing all aging factors is considered difficult and challenging for battery RUL prediction. In general, the application of Li-ion batteries (e.g., HEVs, EVs, or power storage) will determine which aging factors need to be taken into account. The temperature, for instance, released from EV's battery pack during the charging and discharging processes affects battery chemical parameters, which causes the battery pack life to be reduced or degraded.

include relaxation temperature, relaxation SOC, and relaxation time. Next, the performance of the estimated model is examined and compared with real-life battery profiles, followed by the prediction phase.

In the second stage, the battery estimation model is used to predict SOH and RUL using dynamic load profiles (recorded online). During the prediction phase, each battery (*or each battery module that consists of a set of batteries*) measures different battery parameters, including temperature, voltage, current, etc. After that, the capacity degradation of each battery is determined according to its number of cycles, its usage time, or its Ah-throughput (i.e., the quantity of current that passes between electrodes during cycling). For example, the authors of [151] developed a SeM based on an aging dataset for NMC batteries and compared the prediction accuracy of their developed SeM model with various ML models. Based on their simulation results, the SeM performed less well in both the static and dynamic validation tests than the ML models. Although, the SeM model is simpler and easier to construct than the ML models.

### b: EMPIRICAL PREDICTION MODELS WITH FILTERING

In empirical models, the battery parameters are continuously updated as new data becomes available, regardless of whether the data was measured or estimated. In general, aging models are developed by fitting experimental data to a function that accounts for the loss of capacity over time. Most of these models are constructed as functions of the number of cycles or the calendar life with fitted parameters. As well, the behavior of degradation may be described by linear, exponential, or polynomial functions. In our experience, the most usable empirical model for RUL prediction is the double exponential model [132]. For the prediction process to be successful, these parameters (battery aging parameters) must be updated continuously. Due to this, the empirical model is referred to as a *closed-loop model*, meaning the parameters are updated in response to changes in measurement data (i.e., based on feedback). When a new capacity estimate (always using filters) or measurement is available from the BMS, an optimal state estimation method is employed. By using the empirical models with tuned parameters, the RUL may be more accurately predicted after each update.

Empirical models are always associated with the use of filtering algorithms such as the Bayesian filter family, which includes the Kalman filter and particle filter, as well as their variants. By using these filters, a general framework can be developed for modeling dynamic states. With Bayesian estimation, parameters are estimated and updated based on observations using a probability density function (PDF). For this reason, it is important to consider the components of the system and how the noise is distributed when choosing a suitable filter. For *linear systems* with Gaussian noise, Kalman filters (based on the estimation of state-space PDFs) are considered to be the most suitable technique, since the state-space PDF remains Gaussian with each iteration, and the variance of the distribution is propagated through the filter

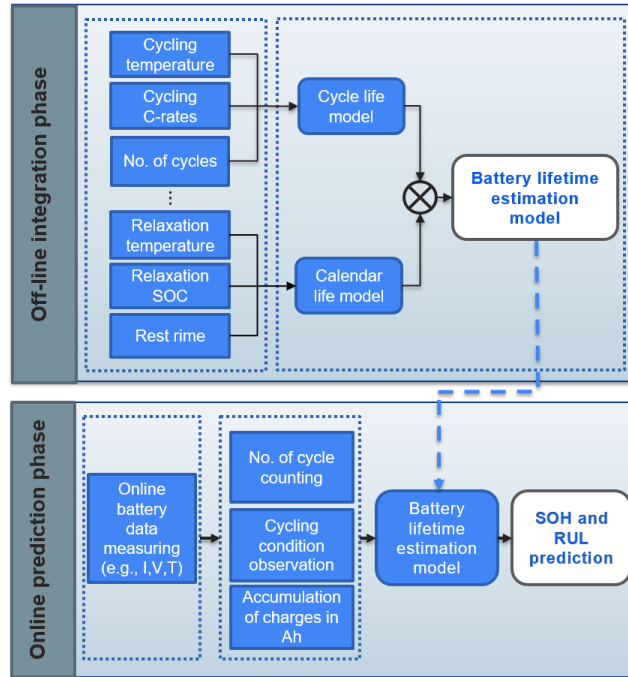


**FIGURE 14.** A generic workflow of the SeM model for RUL prediction, starting from offline integration to online prediction.

Figure 14 illustrates how SeM can be used for online (on-broad) prediction of the RUL. According to this figure, there are two main stages for predicting the RUL: a) the *offline integration phase*, which is associated with constructing the battery lifetime estimation model, and b) the *online prediction phase*, which utilizes the estimation model in predicting the SOH/RUL. Specifically, the offline phase combines the cycle life model with the calendar life model to develop a battery estimation model. As an example, the cycle life model may include cycling temperature, SOC, DOD, C-rate, cycle number, and so on, whereas the calendar life model may

equations [152]. In contrast, Li-ion batteries degrade in a *nonlinear manner*, and during the RUL prediction process, different errors emerge from different sources. As a consequence, the overall noise does not always exhibit Gaussian behavior. As a result, the traditional Kalman filter could diverge under such circumstances. Various algorithms have been developed to address this problem, including extended, sequential, and unscented Kalman filters such as the ones described in [152], [153], [154], and [155] as part of the Kalman filter family.

Particle filter algorithms are also advantageous for dealing with non-Gaussian problems since they take into account the non-linearities of the system, which gives them a distinct advantage. In a sequential Monte Carlo method (e.g., particle filter), Bayesian estimation and importance sampling are incorporated. In other words, based on the Bayesian algorithm, particles with unknown parameters are updated sequentially with parameter probability information. Then, the information acquired in the previous step is utilized at the beginning of this step, and by doing so, updating the parameters by multiplying them by the probability [99]. Several studies, including [156], [157], [158], [159], [160] have used particle filters in predicting the RUL.

## 2) MACHINE LEARNING ALGORITHMS

Although ML algorithms can be used for estimating SOH and predicting RUL, there are significant differences between them in terms of the input features and expected outputs [161]. On the one hand, the BMS collects the input features (e.g., voltage, current, temperature) on-board to estimate the SOH, where the output of the SOH estimator usually represents the capacity for different battery cycles. On the other hand, the use of ML algorithms in predicting the RUL requires a set of capacity values of the SOH estimator as inputs. In other words, the results of the SOH estimation models are used as inputs for the RUL prediction models to predict battery life as a function of cycle count or calendar count (months or years).

ML algorithms can be categorized into three groups: *supervised, unsupervised, and reinforcement learning algorithms*. In supervised learning, the objective is to find a map between input features and outputs with an acceptable degree of accuracy [150]. Additionally, supervised learning can also be divided into two categories: *classification problems* as discrete values (such as failure or non-failure), or *regression problems* as continuous values (such as resistance or capacity values). In other words, classification problems produce categorical output, while regression problems produce real-valued output. In most cases, battery health prediction problems can be classified as regression problems since they produce a numerical value corresponding to the battery's capacity. The unsupervised learning algorithms can make use of given features in order to identify trends or clusters in the data without having an output specified. In reinforcement learning, input/output features do not need to be labeled. Reinforcement learning is simply the process of an intelligent

agent making a series of decisions/actions based on what he sees in the environment using rewards in response to the desired behavior.

In this section, we focus on supervised ML algorithms because the Li-ion battery features and their associated outputs (e.g., capacity) can be measured on-board. It is also possible to classify supervised ML models as follows: a) *non-probabilistic approaches* and b) *probabilistic approaches*. In the first approach, states are related to events rather than describing probabilities, and in the second approach, the uncertainty in predictions is indicated by the distribution of probabilities.

### a: NON-PROBABILISTIC APPROACHES

#### i) AUTO-REGRESSIVE MODEL

Auto-regressive models use past observations of previous time steps to predict future values. Easy parameterization and low computational complexity make the autoregressive model an attractive choice for predicting the RUL. For example, the authors of [162] applied a particle swarm algorithm to optimize an autoregressive model for the prediction of battery capacity degradation. However, when batteries degrade, the fading process becomes nonlinear, thus the autoregressive model will be under-fitted, especially in the context of long-term predictions. To address this problem, a nonlinear autoregressive framework that combines the autoregressive model with moving averages was developed. Through the use of the moving average, the traditional autoregressive model is enhanced by using past prediction errors instead of past prediction values. Another model was proposed by Gou et al. [163], in which a nonlinear autoregressive model was used in conjunction with an ensemble learning structure to improve the stability and accuracy of RUL prediction.

#### ii) ARTIFICIAL NEURAL NETWORKS

In predicting the RUL for Li-ion batteries, a wide variety of ANNs is being utilized, including modular neural network (MNN), FFNN, Kohonen self-organizing neural networks (SONNs), RBF neural networks, HNNs, RNNs, LSTMs, etc. As part of this work, we explain in detail the most useful networks, including FFNNs, RNNs, and HNNs. In general, ANNs simulate the human brain by using artificial neurons (processing units) arranged in three layers: an input layer, an output layer, and a hidden layer. The input layer preprocesses data before redirecting it to the hidden layer(s). Data preprocessing refers to the process of filtering the data that is derived from incomplete battery charging and discharging cycles as well as from data that contains a large amount of noise in order to achieve high accuracy. Each neuron in the hidden layer is represented mathematically by a linear weighted combination coupled with an activation function to determine its output. Accordingly, the more weight a neuron has, the greater its sensitivity will be to the particular input. On the output layer, the model predicts the RUL value according to the input data.

### 1. Feed-Forward Neural Network:

FFNN is considered the simplest ANNs (no loop or feedback) because the data travel in only one direction from the input layer toward the output layer, through the hidden layer. Various researchers have used the FFNN to predict the RUL. For instance, the authors of [123] developed an FFNN model to predict the capacity of Li-ion batteries based on a multi-channel charging profile. They developed and trained their prediction model using the NASA dataset [131]. In their experimental study, they utilized batteries #5, #6, #7, #18 that were charged through the CCCV charging protocol until they reached a maximum voltage of 4.2V. The multi-channel charging profile of these batteries includes voltage, current, and surface temperature which are considered as input to the model, and the capacity data is considered as the model output. Due to the limited size of the available data, they trained the FFNN model by the datasets from batteries #5, #6, #7 and then validated and tested the model with the dataset of battery #18. A key feature of this paper is that it discusses the diversity of feasible data regarding the prediction accuracy of capacity. They compare the prediction accuracy of capacity when the model is trained with single-channel (voltage only) and when it is trained with multi-channel (voltage, current, temperature). Their experimental results showed that prediction accuracy is increased by 58% when using multi-channel data instead of a single channel.

As illustrated in Figure 15, an improved FFNN model is proposed by the authors of [149] which uses cascade forward neural network (CFNN) to predict the RUL. To train and validate their model, they utilized the same experimental environment as in [123] and the same batteries: #5, #6, #7, and #18. The main difference between the CFNN model and the traditional FFNN model is that the CFNN model has a direct connection from the input layer to the output layer. As a result of this direct connection, the CFNN assigns additional weights equal to neuron numbers in the network which results in a faster estimate of the weights. Comparing the CFNN model to the traditional FFNN model, the experimental results showed that the CFNN model has higher accuracy in predicting RUL when using single or multiple-channel input features.

In [164], the authors proposed another ANN model based on applying time-delayed data as an input to the traditional FFNN model to estimate the SOH. This proposed model is referred to as the input time-delayed neural network (ITDNN). As a consequence of the time-delayed inputs, the ITDNN model is more effective to model battery dynamics and memory effects on the battery. Figure 16 depicts the time-delayed voltage, current, and ambient temperature, as inputs to the model, with battery SOH as an output. For the purposes of training and validating their model, they used four milestones from a 20 Ah LFP battery with varying ages (0 h for a fresh battery, 352 h, 544 h, and 650 h for an aged battery). According to their experimental results, the ITDNN model provided better SOH estimation accuracy than the traditional FFNN model. Considering these findings it can be concluded

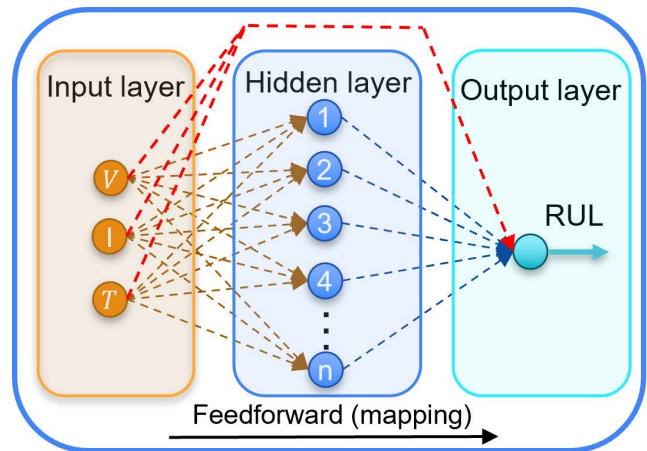


**FIGURE 15.** A representation of cascade forward neural network with 3 input features, 1 hidden layer with  $n$  number of neurons, and 1 output layer [149].

that the use of ITDNN in predicting the RUL may provide better results than either FFNN or CFNN; however, there is no research that has employed this model up to this point.

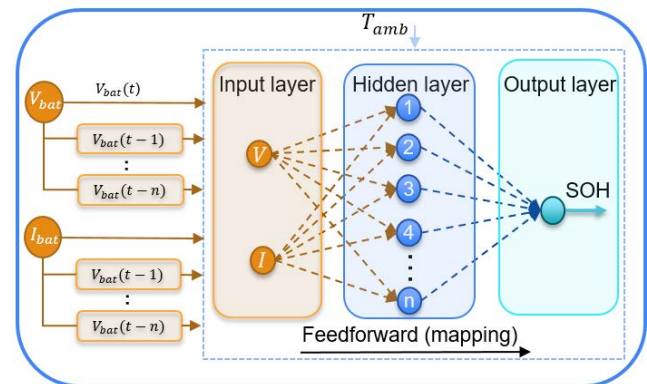


**FIGURE 16.** A simple representation of input time-delayed neural network for SOH estimation [164].

### 2. Recurrent Neural Network:

RNNs are similar to FFNNs but include feedback connectivity between the output layer and the hidden layer, which is shown in Figure 17. In terms of internal memory, the RNN model can process and store past information over a period of time, thereby making it an ideal tool for tracking the correlation between different battery features. Additionally, there is a strong correlation between capacity degradation and battery age, when the batteries are used over hundreds or thousands of cycles. Therefore, extracting and analyzing the correlations is essential in determining the RUL. Based on these considerations, LSTM is a promising type of RNN to capture and update degradation data due to its ability to learn both on short-term and long-term scales.

According to [123] as discussed previously, the authors also constructed an LSTM model to predict the RUL and compared its prediction accuracy to the FFNN model. Based on their experimental results, LSTM is more accurate in

predicting RUL than FFNN. Furthermore, they demonstrated that using multi-channel data instead of single-channel data can improve the accuracy of LSTM by 25%. A hybrid approach combining an ML model and a physical model is proposed in [165] to increase the accuracy of RUL predictions for Li-ion batteries using the RNN model and state-space estimation methods, which are typical of filtering-based techniques. For the training of the RNN, a large dataset is generated with the state-space estimation procedure. The condition monitoring unit provides data on the battery's internal capacity, and these data are used to estimate the battery's SOC. This newly generated data is then used to train the RNN model. In the corresponding RNN model, a genetic algorithm is used to optimize the model using additional deep layers in order to improve predictions of the nonlinear trend of battery levels. The NASA battery dataset of batteries #5, #6, #7, and #18 has been also used to assess the performance of their proposed method. In addition, they examined two degradation models, a well-known empirical double exponential model and a new single exponential model, which is capable of ensuring optimal performance with fewer estimation parameters. Furthermore, they compare the predictions of their model to a state-of-the-art, demonstrating that their model performs optimally in terms of RUL prediction. Generally, it can be observed that the feedback between the hidden and output layers of the RNN model can increase the accuracy of the RUL prediction. Several other research studies that employ RNNs, LSTMs, or a hybrid model can be found in [166], [167], [168], [169], and [170].

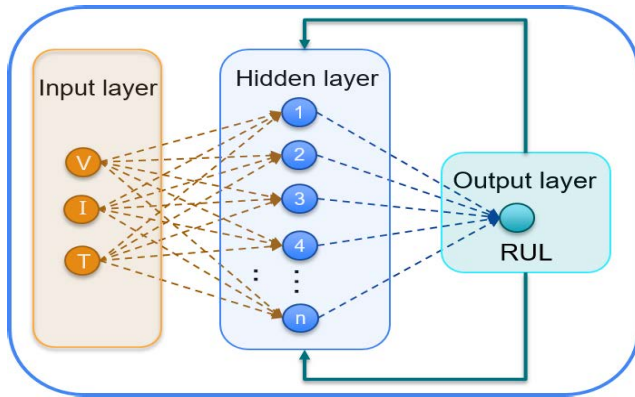


**FIGURE 17.** A simple representation of an RNN with 3 input features, 1 hidden layer with  $n$  number of neurons, and 1 output layer.

### 3. Hamming Neural Network

An HNN model can be thought of as a combination of the FFNN model and the RNN model. In [171], a dual extended Kalman filter was employed in conjunction with an HNN model in order to identify the battery parameters of ECM (first-order ECM) with the objective of achieving high estimation accuracy for SOH. Specifically, HNN estimates of ECM battery parameters are presented based on three patterns: capacity patterns, charge-discharge voltage patterns, and changes in those patterns over time. Following the identification of battery parameters, the dual extended Kalman

filter is used to estimate SOH. The dataset patterns used to develop and validate this model are divided into 15 different categories. To make the data suitable for use in an HNN, a binary array must be created with elements of -1 or 1. When the HNN model has identified the predetermined pattern closest to an arbitrarily selected battery, the ECM battery parameters corresponding to the selected pattern are then identified. Based on their experimental results, the developed model can correctly identify battery ECM model parameters without having to repeat battery parameter measurements. This study, however, is limited to one temperature setting of 27°C, and no further investigation has been conducted to predict the RUL using this model. Therefore, more attention is needed to utilize this model in predicting the RUL, which could have better accuracy than the previous state-of-the-art.

### b: PROBABILISTIC APPROACHES

Considering the non-linearity in Li-ion battery parameters, as well as the uncertainties in measurement procedure and operating environment, the prediction models of RUL should account for these uncertainties for better accuracy. For this reason, probabilistic approaches have been developed to reflect all of these types of uncertainty by identifying unknown uncertainty and its relationship with the data through probabilistic distributions [172], [173].

#### i) GAUSSIAN PROCESS REGRESSION

Models based on GPR can be used to predict RUL using their flexible, non-parametric, and probabilistic techniques that are very useful for predictions [174]. In GPR, a Bayesian kernel is used to encapsulate historical knowledge and provide predictions. The authors of [175] described residual variances that are associated with average predictions for various scenarios as a function of uncertainty. Therefore, Gaussian processes can be viewed as a group of random variables with joint multivariate Gaussian distributions [174], [176]. Based on the level of degradation in battery capacity that occurs during battery operation, the authors of [177] proposed a GPR model with multiple outputs to predict SOH as well as RUL for Li-ion batteries. Their model was trained and validated using the NASA dataset for batteries number #1, #2, and #4, which were captured from a charging/discharging of a 0.9 Ah Li-ion battery. The experimental results showed that multiple-output models tended to perform better when extracting data from multiple batteries, resulting in highly accurate predictions of RUL. Nevertheless, this model has a *high computational complexity* when dealing with multiple or large numbers of outputs. They further developed an enhanced GPR transition model [178] for describing the mappings between diverse current, voltage, temperature, and capacity with an aim to predict battery degradation. In contrast to this model, the basic GPR method does not detect the local regeneration that occurs when a battery shows abrupt and temporary increases in capacity during capacity degradation. In the GPR model, co-variance functions and mean functions are combined for multi-step-ahead prognostics [117].

GPR's prediction accuracy is high in response to the covariance function, which means the kernels must be selected carefully due to the complex nature of capacity fading (as many factors contribute to it) [176]. In the case of non-linear mappings involving multi-channel input features, a single co-variance function would result in unreliable predictions [174]. Thus, advanced structures such as automatic relevance determination [179] should be used for constructing an isotropic kernel. Overfitting may result when hyperparameters in the co-variance function are not optimized appropriately. In developing the GPR model, this problem can be solved by reducing the negative logarithmic marginal likelihood [176].

According to [151], the authors developed three different ML algorithms, including GPR, nonlinear autoregressive with exogenous input (NARX), and SeM to predict RUL. In comparison with the GPR model, the NARX model shows a lower RMSE for both static and dynamic validation as well as a lower training time, while the SeM model shows a higher RMSE but requires less time for training.

#### *ii) RELEVANCE VECTOR MACHINE*

RVM method is originally introduced by Tipping [180], it is similar to the SVM algorithm but based on probabilistic principles. Using the RVM, PDFs of the outputs can be obtained instead of point estimates (classification) by estimating the weights of the Bayesian network. Despite using kernel functions with high sparsity, RVM has comparable performance to SVM and provides probabilistic predictions [181]. It is important to note that sparsity occurs when a large proportion of weights have zero values, which results in more efficient models.

Several studies have shown that RVM is a powerful tool for predicting RUL because of its ability to deal with uncertainty. According to the model proposed by the authors of [182], the RVM is capable of producing relevance vectors that can be used to predict future battery capacity degradation. An uncertainty model is used for determining the parameters of a capacity degradation based on the prediction of degradation values. In that article, the authors used a wavelet denoising method to reduce the model uncertainty and calculate the historical information. In addition, the RVM model is employed as a nonlinear time series for predicting the battery's remaining life. A further incremental approach for online learning was proposed by the authors of [183] to improve the prediction accuracy of the RVM model for long-term RUL prediction. According to their findings, the RVM achieved a high degree of precision, excellent learning capabilities, simple training procedures, and accurate prediction results with a high probability level. RVM model, however, has a major disadvantage of requiring large datasets for training, resulting in significant computational and memory expenses.

## VIII. PERFORMANCE TESTS

For the purpose of estimating battery SOH or RUL using ML models, an acceptable quantity and quality of data are

required. However, collecting the battery aging data is an exhausting process of experiments designed to gather sufficient battery information that represents the entire battery life. Furthermore, it would be challenging to repeat these experiments because they would require a large amount of time and money. Thus, the collection of a high-performance battery dataset can take up to several years.

In this section, one of the most valuable battery degradation datasets in this line of research, the NASA battery degradation dataset, is used to train and validate three ML algorithms, including SVR, FFNN, and LSTM. NASA dataset contains three different operational profiles: charge, discharge, and impedance at different ambient temperatures for various Li-ion batteries from their BOL until they reached their EOL. Initially, the battery voltage was charged in a constant current mode at 1.5 A until 4.2 V was reached, then in a constant voltage mode until the current dropped to 20 mA. Batteries were deemed to be obsolete (EOL) when their capacity failed by 30% from its fresh value (i.e., dropped from 2 Ah to 1.4 Ah). In this work, we first extract the features from this dataset, particularly from the discharge profile. Next, we process and filter the dataset by removing the redundant data. Finally, we use the pre-processed data to estimate the SOH. Following is an explanation for the extraction of features and filtering of the NASA dataset during the discharge profile.

### A. DISCHARGE PROFILE OF NASA DATASET

Prior to developing an ML model, we need to analyze the battery discharge profile which has three sub-profiles: *voltage profile*, *current profile*, and *temperature profile*, each of which will serve as an input feature to train our ML algorithms. For labeling these input features, the measured battery capacity of each cycle from the battery's BOL to its EOL will be utilized. Figures 18 and 19 depict the voltage, current, and temperature profiles as well as the degradation curve of the battery capacity during the battery discharge phase for battery number #5, as documented by NASA's dataset, at ambient temperature 25°C.

### B. FEATURE EXTRACTION OF DISCHARGE PROFILE

During the discharge process, the size of the samples collected is affected by the battery life. More specifically, each discharge cycle contains different numbers of data samples, where the fresh battery may have 5000 samples, but an aged battery may only have 700 samples. For this reason, raw data must be processed to extract key characteristics from the data of each battery cycle before being integrated into the feature fusion model. Generally, a better SOH estimation can be achieved through the extraction of more key features from raw data.

To solve the problem of varying sample sizes, it is logical to take the same sample points at equal intervals during each battery cycle. The easiest way to do this is to discard some points in each cycle. This way, however, does not produce satisfactory results due to the non-linearity degradation of the battery data. For this reason, it is essential to determine

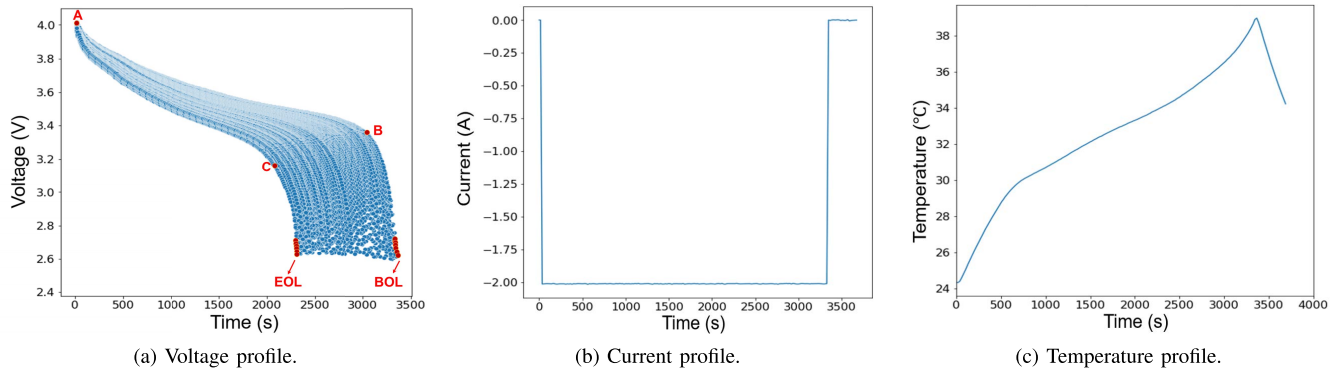


**FIGURE 18.** An example of a Li-ion battery discharge profile (battery #5 in NASA's dataset), in which (a) shows voltage curves from the battery's BOL to its EOL, (b) and (c) show the profiles of current and temperature, respectively, for one complete cycle.

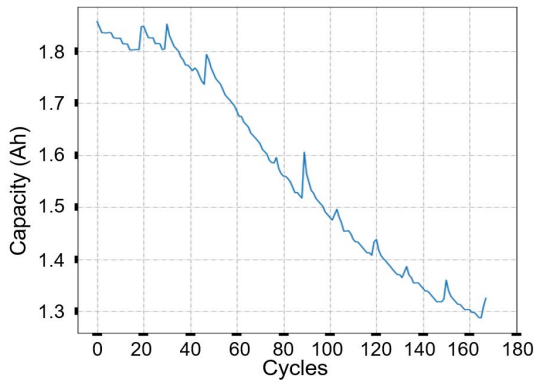


**FIGURE 19.** The capacity curve of Li-ion battery number #5 during a discharge phase from its BOL to its EOL.

a reliable way to extract the battery features in order to have sufficient and effective sample points. Specifically, for each characteristic of the Li-ion Battery, there are very clear geometric patterns, which are highly dependent on the battery decay. As a result, we can extract typical key characteristics for each of the discharge cycles and use them to characterize the current state of Li-ion batteries.

Figure 18a illustrates the voltage profile of battery number #5 at its BOL and EOL. As shown from this figure, it is hard to determine which points should be included in estimating the SOH and which should be discarded. On the other hand, if we consider the points such as A, B, and C which represent the degradation of voltage gradient with regard to different ages of batteries, the problem of non-linearity in battery data can be overcome. Therefore, it is important to consider a number of key points that may represent a difference between the battery at different ages as they influence the battery's performance.

After processing the input features, we train three ML models, FFNN, SVR, and LSTM, and compare their performance in estimating battery SOH. For a fair comparison between these battery models, the same training parameters (number of layers, number of epochs, number of

neurons, etc.) were employed. The following considerations apply to all ML algorithms used:

- Each ML algorithm is composed of one input layer, two hidden layers, and one output layer.
- Training parameters are: epochs=500, batches=32, loss function=mean\_squared\_error, optimizer=ADAM, metrics=accuracy.
- Each battery is trained and tested with the same training/testing ratio 80-20 %.

Additionally, testing was performed using Python 3.9 on a platform with a processor of Intel(R) Core (TM) i7-CPU Q720 at 1.6 GHz and memory (RAM) of 4.00 GB. In order to label input features with the corresponding SOH, the SOH of the battery is determined based on the following equation:

$$SOH\% = \frac{C_c}{C_{nom}} * 100\% \quad (8)$$

where  $C_c$  is the capacity of the battery at each cycle, and  $C_{nom}$  denotes the battery nominal capacity at BOL which is given in the dataset for each battery. Below is the RMSE equation used in our evaluation:

$$RMSE\% = \sqrt{\frac{1}{N} \sum_{i=1}^N \left[ \frac{SOH_c - SOH_e}{SOH_c} \right]^2} * 100\% \quad (9)$$

where the number  $N$  denotes the number of sample points,  $SOH_c$  is the determined SOH as shown in (8), and  $SOH_e$  is the estimated battery SOH derived from the testing of our model. It is worth noting that the lower the RMSE, the better the accuracy of the battery model.

### C. RESULTS DISCUSSION

The experiment was repeated and initially produced satisfactory results in some cases. Following additional experiments, the results have become stable. Figure 20 shows the results of estimating battery SOH using the FFNN algorithm for batteries #5, #6, and #7. As shown in the figure, the horizontal axis represents the number of cycles a battery goes through from its BOL until reaching its EOL, while the vertical axis represents a percentage estimate of battery life. In this figure, the lowest SOH value of the battery is 58%, where the battery

reached the end of its *first life* for on-board applications and must retire and start its *second life* off-board. Additionally, the figure shows that the difference between the measured and the estimated values of SOH is relatively small for batteries #5, and #6, but it is slightly larger for battery #7.

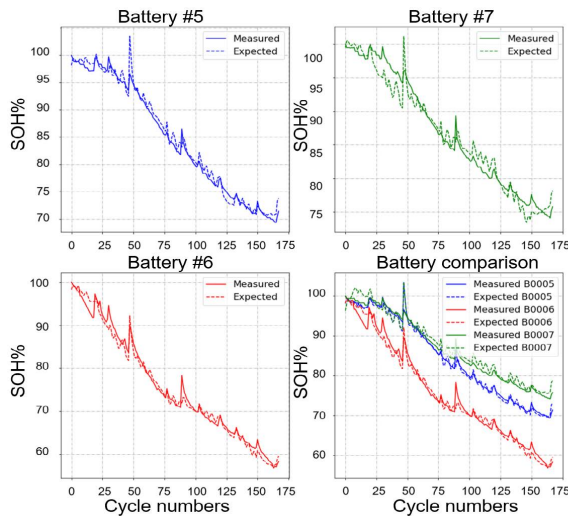


**FIGURE 20.** Comparison of SOH using FFNN algorithm in modeling Li-ion batteries based on NASA datasets of batteries #5, #6, and #7.

Figure 21 shows the estimations of SOH for batteries #5, #6, and #7 using the SVR algorithm. According to this figure, the difference between the calculated and estimated SOH values for batteries #5 and #6 is still within acceptable limits. On the other hand, the difference between the measured and estimated value of SOH is increased for battery #7, especially at the first fifty cycles, indicating that the dataset for this battery is not very accurate in comparison to other batteries. An important consideration is that the quality of the dataset

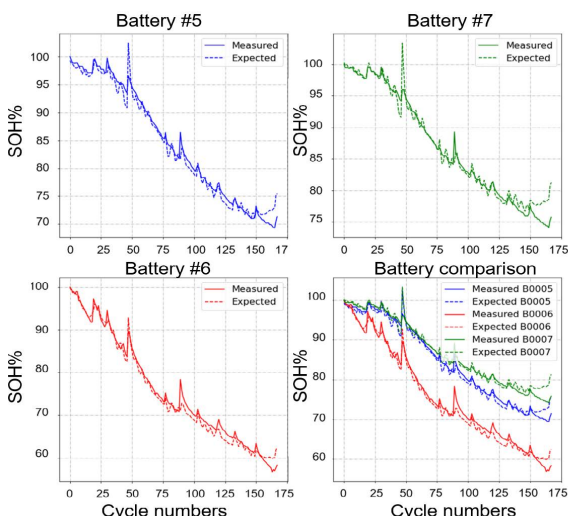


**FIGURE 21.** Comparison of SOH using SVR algorithm in modeling Li-ion batteries based on NASA datasets of batteries #5, #6, and #7.

is crucial to the accuracy of the ML algorithm in estimating battery health.

Figure 22 depicts the SOH estimation for batteries #5, #6, and #7 using LSTM algorithm. According to this figure, the difference between the measured and estimated battery SOH values for batteries #5 and #6 is very small when compared to the FFNN and SVR algorithms. Although, the large difference between the measured and estimated battery SOH value for battery #7 is reduced and becomes an acceptable range compared to previously mentioned algorithms. This improvement in estimation accuracy was expected since the LSTM algorithm estimates the next value by looking at the past as well as the present. Therefore, even though the dataset's accuracy is not very high, the estimated value can have good accuracy. In comparison to FFNN or SVR, the LSTM algorithm is more complex and requires more training time.

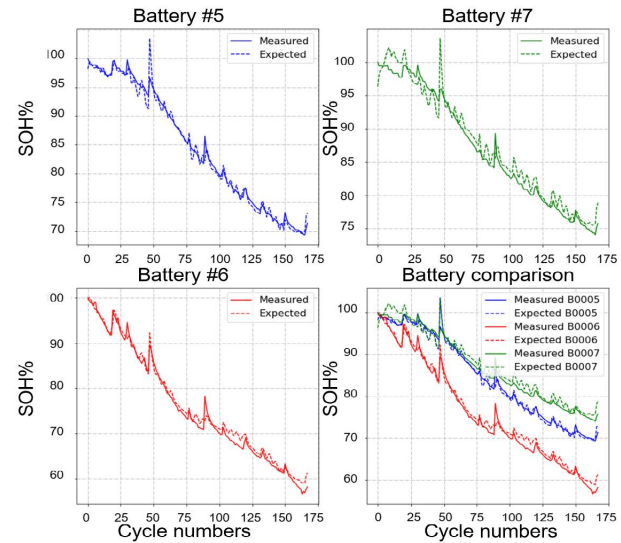


**FIGURE 22.** Comparison of SOH using LSTM algorithm in modeling Li-ion batteries based on NASA datasets of batteries #5, #6, and #7.

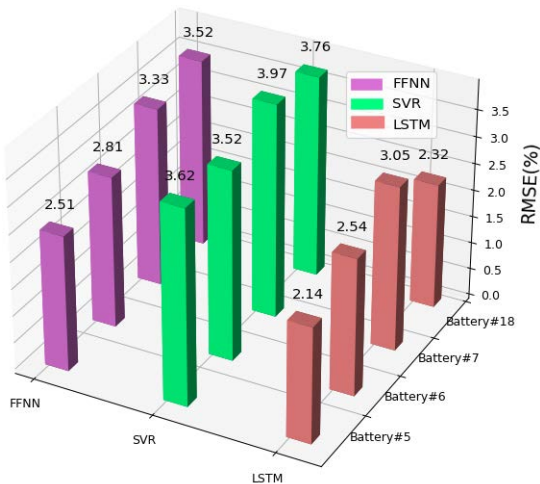
#### D. BENCHMARK

Table 6 and Figure 23 summarize the results for SOH estimation using FFNN, SVR, and LSTM algorithms in modeling batteries number #5, #6, #7, and #18 as numbered in NASA dataset. In comparison with SVR and FFNN, the LSTM algorithm has the lowest RMSE, therefore it is the most accurate algorithm when estimating battery SOH. In spite of this, the RMSE difference between these three models is around 1.5%, which is not significantly different when considering that the

**TABLE 6.** The RMSE% for various battery SOH estimation models.

	Battery#5	Battery#6	Battery#7	Battery#18
FFNN	2.51%	2.81%	3.33%	3.52%
SVR	3.62%	3.52%	3.97%	3.76%
LSTM	2.14%	2.54%	3.05%	2.32%

LSTM is more complex than the other two models. As a result, there can be a trade-off between model complexity and accuracy.



**FIGURE 23.** Comparison of different ML models (FFNN, SVR, and LSTM) in terms of SOH with respect to RMSE%.

Although LSTMs demonstrate acceptable SOH estimation accuracy, they are based on the degradation dataset used, meaning that traditional models are not robust enough when used with dynamic battery data. In order to improve the estimation accuracy and enhance the robustness of ML models, the researchers developed hybrid models. For instance, the authors of [163] developed a hybrid ML algorithm that combines ELM and random vector functional link (RVFL) to estimate SOH and predict the RUL of Li-ion batteries. Their proposed model was also trained and tested using the NASA dataset. Additionally, they compared their hybrid model with a variety of ML models, including stacked denoising autoencoders (SDA), SVM, echo state networks (ESN), random forest (RF), RVFL, and ELM. They proved that the combined ELM&RVFL model offers the lowest RMSE value in comparison to the other models as well as is more robust when they tested it under different datasets.

NARX model with embedded LSTM is another hybrid ML mode proposed by [184], which incorporates jump-ahead connections in the time-unfolded model. These jump-ahead connections reduce long-term dependence on the RNN by providing a shorter path for gradient information to propagate. They validated their model using urban dynamometer driving schedules and dynamic stress tests. The experimental results presented in [184] showed that the NARX-LSTM model has the smallest RMSE 0.76% and 0.78% using two different datasets, whereas the traditional LSTM has a greater RMSE which is 1.87% and 1.95% using the same dataset and parameters.

Through this section, we presented a comparison between various ML models used to estimate the SOH. As shown in this comparison, hybrid algorithms produce higher accuracy than a single ML algorithm in estimating SOH.

Unfortunately, these models have some gaps due to their dependency on the quality of the datasets, which affects the robustness of SOH estimation. As most of these datasets were collected in laboratories, the performance of these models does not reflect real-world applications. Further, these datasets typically measure only the current, voltage, and temperature of batteries, which may not provide sufficient information about how batteries perform over time. Consequently, enhancements are necessary to fill these gaps.

## IX. BENCHMARK OF BATTERY HEALTH PREDICTION TECHNIQUES

A variety of methods are developed to estimate and predict battery health. All prediction methods are aiming to achieve a high degree of accuracy, however, no single strategy has been developed to address all the current challenges. For each individual application like EVs or HEVs, the suggested model attempts to strike a balance between *accuracy*, *computational effort*, *complexity*, and *applicability*. Figure 24 illustrates a comparison between various techniques for battery RUL prediction. According to our analysis, the data-driven models had high applicability and performance, making them useful for on-board battery life prediction. Nevertheless, these methods are limited by their high level of computational efforts, which is considered the main drawback of these methods. *In fact, there is no straightforward method for selecting the best battery health prediction method.* The selection of the most appropriate prediction method depends on the given application, the information available about the battery parameters, and the quality of the dataset.

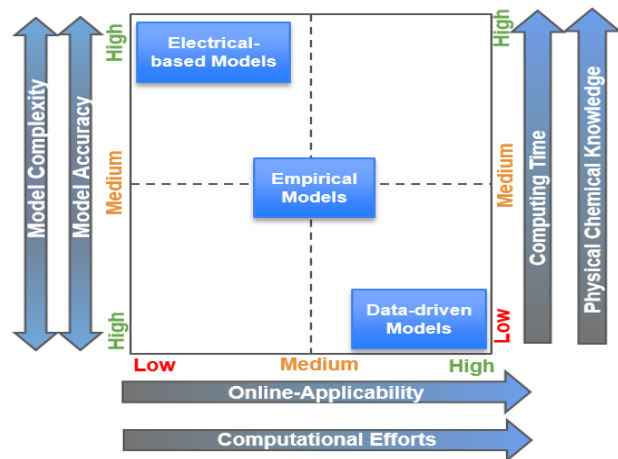


**FIGURE 24.** Comparison between different battery lifetime prediction models.

In Figure 25, a framework of the complete estimation and prediction processes is shown in conjunction with the BMS for EVs as a real-world application. In this framework, data-driven models are considered for estimating and predicting battery health thanks to their high applicability for onboard applications. There are three main phases in this framework: a) diagnostic phase, b) prognostic phase, and c) maintenance

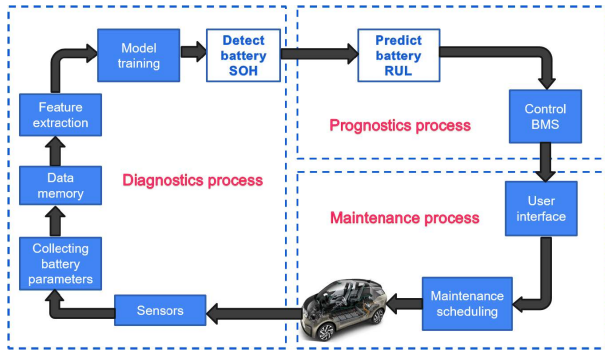


**FIGURE 25.** The diagnosis, prognosis, and maintenance processes of Li-ion batteries in EVs based on ML algorithms.

phase. During the first phase, the installed sensors measure and record battery external parameters. After that, the data will be stored in a memory to be used as a historical dataset in the future. The next step would be to extract features from the dataset that would contain information about the battery age. Next, the ML model is created and trained using this available dataset. In the final stage of this process, the battery SOH estimation is determined as the estimated output. It is important to emphasize that during the battery life, the data collection process continues in order to increase the model's accuracy. The second phase of the RUL prediction utilizes the output from the estimation process as an input to the battery RUL predictor. Following this, the output of the battery RUL predictor is sent directly to the BMS to improve battery performance. During the maintenance process phase, the battery health status will be displayed for the user on the graphical interface. In the event of worsening battery health or the need to retire the battery, the user will schedule an auto maintenance appointment to replace or repair the battery.

## X. CONCLUSION AND RECOMMENDATION

The main objective of this paper was to review and discuss the health status of EV batteries to ensure their operational safety. For this purpose, various battery modeling techniques were discussed. Two main approaches have been proposed in the literature: *physically-based approach* and *data-driven approach*. In the physically-based approach, the most comprehensive and accurate model is the electrochemical model which consists of a set of partial differential equations. Unfortunately, this model is complex and may not be used to monitor the battery's health in real-time applications. Further research is needed to achieve an acceptable compromise between model complexity and accuracy. In the data-driven model, the model parameters are not known directly, but relevant model information is determined using ML algorithms and training data. Even though this modeling approach is simple to use, its accuracy mainly depends on the amount of training data, and the ML algorithm used. Nevertheless, obtaining the proper amount of data is challenging. In addition, there is no universal ML model that can be used to estimate battery health with a high level of accuracy. Further research is needed to find a compromise between the model accuracy,

and ML algorithm complexity. A performance comparison between physical and data-driven modeling approaches using the same battery and the same operating conditions will be useful. It is worth considering the use of deep learning neural networks that can be trained during vehicle operation. Given an accurate model, battery SOH and RUL prediction can be achieved to ensure the safety of the use of EV batteries. Also, to provide a fair and accurate comparison between the different data-driven models, a generalized validation test is needed for estimating battery health.

## REFERENCES

- [1] X. Hu, C. Zou, C. Zhang, and Y. Li, "Technological developments in batteries: A survey of principal roles, types, and management needs," *IEEE Power Energy Mag.*, vol. 15, no. 5, pp. 20–31, Sep. 2017.
- [2] M. A. Hannan, M. M. Hoque, A. Hussain, Y. Yusof, and P. J. Ker, "State-of-the-art and energy management system of lithium-ion batteries in electric vehicle applications: Issues and recommendations," *IEEE Access*, vol. 6, pp. 19362–19378, 2018.
- [3] D. A. Wetz, B. Shrestha, S. T. Donahue, D. N. Wong, M. J. Martin, and J. Heinzel, "Capacity fade of 26650 lithium-ion phosphate batteries considered for use within a pulsed-power system's prime power supply," *IEEE Trans. Plasma Sci.*, vol. 43, no. 5, pp. 1448–1455, May 2015.
- [4] A. Allam and S. Onori, "Online capacity estimation for lithium-ion battery cells via an electrochemical model-based adaptive interconnected observer," *IEEE Trans. Control Syst. Technol.*, vol. 29, no. 4, pp. 1636–1651, Jul. 2021.
- [5] A. Farmann, W. Waag, A. Marongiu, and D. U. Sauer, "Critical review of on-board capacity estimation techniques for lithium-ion batteries in electric and hybrid electric vehicles," *J. Power Sources*, vol. 281, pp. 114–130, May 2015.
- [6] L. Fred. (Jun. 2021). *Brand New Tesla Model S Plaid Caught on Fire in Strange Circumstances*. Accessed: Jul. 22, 2021. [Online]. Available: <https://electrek.co/2021/06/30/tesla-model-s-plaid-caught-fire-strange-circumstances/>
- [7] National Transportation Safety Board, Washington, DC, USA. (Nov. 2020). *Safety Risks to Emergency Responders From Lithium-Ion Battery Fires in Electric Vehicles*. Accessed: Jul. 21, 2021. [Online]. Available: <https://www.ntsb.gov/safety/safety-studies/Documents/SR2001/pdf>
- [8] N. Gabriel. (Mar. 2019). *BMW i8 Catches Fire, Gets Dunked in Water*. Accessed: Jul. 22, 2021. [Online]. Available: <https://www.bmwblog.com/2019/03/26/bmw-i8-caught-fire-gets-dunked-in-water/>
- [9] (Jul. 2020). *US Investigates Fire Reports in Chevy Bolt Electric Vehicles*. Accessed: Jul. 22, 2021. [Online]. Available: <https://abcnews.go.com/US/wireStory/us-investigates-fire-reports-chevy-bolt-electric-vehicles-73582418>
- [10] G. Sean. (May 2021). *Chevy Bolt Fire Just Days After Fix Announced*. Accessed: Jul. 25, 2021. [Online]. Available: <https://electrek.co/2021/05/03/another-devastating-chevy-bolt-fire-just-days-after-fix-announced/>
- [11] R. Kshitij. (Jun. 2021). *Two Reports of Hyundai Kona EVs Spontaneously Bursting Into Flames Have Emerged, One From South Korea and the Other From Norway*. Accessed: Jul. 25, 2021. [Online]. Available: <https://tinyurl.com/u588bn88>
- [12] G. Will. (Oct. 2020). *Electric Vehicle Thought to Have Caught Fire in Garage*. Accessed: Jul. 25, 2021. [Online]. Available: <https://tinyurl.com/panne8nv>
- [13] K. Mak. (Oct. 2020). *While Charging the Battery of Kona EV Fires Again in Namyangju*. Accessed: Jul. 25, 2021. [Online]. Available: <https://tinyurl.com/yuh9cw7>
- [14] K. Mark. *Watch Opel Ampera-e Catch Fire in Germany*. Accessed: Jul. 25, 2021. [Online]. Available: <https://insideevs.com/news/452410/watch-opel-ampera-e-fire-germany-video/>
- [15] P. Sun, R. Bisschop, H. Niu, and X. Huang, "A review of battery fires in electric vehicles," *Fire Technol.*, vol. 56, pp. 1361–1410, Jan. 2020.
- [16] (Jul. 2021). *Tesla Top-of-Range Car Caught Fire While Owner Was Driving, Lawyer Says*. Accessed: Jul. 22, 2021. [Online]. Available: <https://www.reuters.com/business/autos-transportation/tesla-top-of-range-car-caught-fire-while-owner-was-driving-lawyer-says-2021-07-02/>

- [17] (May 2018). *Preliminary Report: Highway HWY18FH013*. Accessed: Jul. 22, 2021. [Online]. Available: <https://www.ntsb.gov/investigations/AccidentReports/Pages/HWY18FH013-prelim.aspx>
- [18] J. Revill. (May 2018). *Tesla Crash May Have Triggered Battery Fire: Swiss Firefighters*. Accessed: Jul. 22, 2021. [Online]. Available: <https://www.autoblog.com/2018/05/14/tesla-crash-fire-switzerland/>
- [19] O. Erik. (Apr. 2021). *Electric Vehicle Fires are Rare, but Challenging to Extinguish*. Accessed: Jul. 22, 2021. [Online]. Available: <https://www.popsci.com/story/technology/electric-vehicle-battery-tesla-fire/>
- [20] Y. Gao, K. Liu, C. Zhu, X. Zhang, and D. Zhang, "Co-estimation of state-of-charge and state-of-health for lithium-ion batteries using an enhanced electrochemical model," *IEEE Trans. Ind. Electron.*, vol. 69, no. 3, pp. 2684–2696, Mar. 2022.
- [21] K. S. Hariharan, P. Tagade, and S. Ramachandran, *Mathematical Modeling of Lithium Batteries: From Electrochemical Models to State Estimator Algorithms* (Green Energy and Technology). Cham, Switzerland: Springer, 2017, doi: [10.1007/978-3-319-03527-7](https://doi.org/10.1007/978-3-319-03527-7).
- [22] R. Xiong, "Modeling theory of lithium-ion batteries," in *Battery Management Algorithm for Electric Vehicles*. Singapore: Springer, 2020, pp. 63–106.
- [23] F. Zhu and J. Fu, "A novel state-of-health estimation for lithium-ion battery via unscented Kalman filter and improved unscented particle filter," *IEEE Sensors J.*, vol. 21, no. 22, pp. 25449–25456, Nov. 2021.
- [24] L. Ling and Y. Wei, "State-of-charge and state-of-health estimation for lithium-ion batteries based on dual fractional-order extended Kalman filter and online parameter identification," *IEEE Access*, vol. 9, pp. 47588–47602, 2021.
- [25] R. Xiong, J. Cao, Q. Yu, H. He, and F. Sun, "Critical review on the battery state of charge estimation methods for electric vehicles," *IEEE Access*, vol. 6, pp. 1832–1843, 2017.
- [26] M. A. Hannan, M. S. H. Lipu, A. Hussain, and A. Mohamed, "A review of lithium-ion battery state of charge estimation and management system in electric vehicle applications: Challenges and recommendations," *Renew. Sustain. Energy Rev.*, vol. 78, pp. 834–854, Oct. 2017.
- [27] M.-F. Ge, Y. Liu, X. Jiang, and J. Liu, "A review on state of health estimations and remaining useful life prognostics of lithium-ion batteries," *Measurement*, vol. 174, Apr. 2021, Art. no. 109057.
- [28] S. Yang, C. Zhang, J. Jiang, W. Zhang, L. Zhang, and Y. Wang, "Review on state-of-health of lithium-ion batteries: Characterizations, estimations and applications," *J. Cleaner Prod.*, vol. 314, Sep. 2021, Art. no. 128015.
- [29] A. Basia, Z. Simeu-Abazi, E. Gascard, and P. Zwolinski, "Review on state of health estimation methodologies for lithium-ion batteries in the context of circular economy," *CIRP J. Manuf. Sci. Technol.*, vol. 32, pp. 517–528, Jan. 2021.
- [30] R. Xiong, Y. Zhang, H. He, S. Peng, M. Pecht, and J. Wang, "Lithium-ion battery health prognosis based on a real battery management system used in electric vehicles," *IEEE Trans. Veh. Technol.*, vol. 68, no. 5, pp. 4110–4121, May 2019.
- [31] Y. Li, K. Liu, A. M. Foley, A. Zülke, M. Berecibar, E. Nanini-Maury, J. Van Mierlo, and H. E. Hoster, "Data-driven health estimation and lifetime prediction of lithium-ion batteries: A review," *Renew. Sustain. Energy Rev.*, vol. 113, Oct. 2019, Art. no. 109254.
- [32] C. Vidal, P. Malysz, P. Kollmeyer, and A. Emadi, "Machine learning applied to electrified vehicle battery state of charge and state of health estimation: State-of-the-art," *IEEE Access*, vol. 8, pp. 52796–52814, 2020.
- [33] D. N. How, M. A. Hannan, M. H. Lipu, and P. J. Ker, "State of charge estimation for lithium-ion batteries using model-based and data-driven methods: A review," *IEEE Access*, vol. 7, pp. 136116–136136, 2019.
- [34] W. Liu, Y. Xu, and X. Feng, "A hierarchical and flexible data-driven method for online state-of-health estimation of Li-ion battery," *IEEE Trans. Veh. Technol.*, vol. 69, no. 12, pp. 14739–14748, Dec. 2020.
- [35] B. Zraibi, C. Okar, H. Chaoui, and M. Mansouri, "Remaining useful life assessment for lithium-ion batteries using CNN-LSTM-DNN hybrid method," *IEEE Trans. Veh. Technol.*, vol. 70, no. 5, pp. 4252–4261, May 2021.
- [36] Y. Wang, Y. Ni, S. Lu, J. Wang, and X. Zhang, "Remaining useful life prediction of lithium-ion batteries using support vector regression optimized by artificial bee colony," *IEEE Trans. Veh. Technol.*, vol. 68, no. 10, pp. 9543–9553, Oct. 2019.
- [37] D. Zhou, Z. Li, J. Zhu, H. Zhang, and L. Hou, "State of health monitoring and remaining useful life prediction of lithium-ion batteries based on temporal convolutional network," *IEEE Access*, vol. 8, pp. 53307–53320, 2020.
- [38] J. Wei, G. Dong, and Z. Chen, "Remaining useful life prediction and state of health diagnosis for lithium-ion batteries using particle filter and support vector regression," *IEEE Trans. Ind. Electron.*, vol. 65, no. 7, pp. 5634–5643, Jul. 2018.
- [39] X. Hu, Y. Zheng, X. Lin, and Y. Xie, "Optimal multistage charging of NCA/graphite lithium-ion batteries based on electrothermal-aging dynamics," *IEEE Trans. Transport. Electrific.*, vol. 6, no. 2, pp. 427–438, Jun. 2020.
- [40] Z. Wang, J. Ma, and L. Zhang, "State-of-health estimation for lithium-ion batteries based on the multi-island genetic algorithm and the Gaussian process regression," *IEEE Access*, vol. 5, pp. 21286–21295, 2017.
- [41] M. J. Brand, M. H. Hofmann, S. F. Schuster, P. Keil, and A. Jossen, "The influence of current ripples on the lifetime of lithium-ion batteries," *IEEE Trans. Veh. Technol.*, vol. 67, no. 11, pp. 10438–10445, Nov. 2018.
- [42] M. A. Roscher and D. U. Sauer, "Dynamic electric behavior and open-circuit-voltage modeling of LiFePO<sub>4</sub>-based lithium ion secondary batteries," *J. Power Sources*, vol. 196, no. 1, pp. 331–336, Jan. 2011.
- [43] Z. Liu, X. Dang, and B. Jing, "A novel open circuit voltage based state of charge estimation for lithium-ion battery by multi-innovation Kalman filter," *IEEE Access*, vol. 7, pp. 49432–49447, 2019.
- [44] D.-I. Stroe, V. Knap, M. Swierczynski, and E. Schaltz, "Electrochemical impedance spectroscopy-based electric circuit modeling of lithium-sulfur batteries during a discharging state," *IEEE Trans. Ind. Appl.*, vol. 55, no. 1, pp. 631–637, Jan. 2019.
- [45] M. Doyle, T. F. Fuller, and J. Newman, "Modeling of galvanostatic charge and discharge of the lithium/polymer/insertion cell," *J. Electrochem. Soc.*, vol. 140, no. 6, p. 1526, 1993.
- [46] A. Bartlett, J. Marcicki, S. Onori, G. Rizzoni, X. G. Yang, and T. Miller, "Electrochemical model-based state of charge and capacity estimation for a composite electrode lithium-ion battery," *IEEE Trans. Control Syst. Technol.*, vol. 24, no. 2, pp. 384–399, Mar. 2016.
- [47] C. Zou, C. Manzie, and D. Nešić, "A framework for simplification of PDE-based lithium-ion battery models," *IEEE Trans. Control Syst. Technol.*, vol. 24, no. 5, pp. 1594–1609, Sep. 2016.
- [48] Z. Song, H. Wang, J. Hou, H. F. Hofmann, and J. Sun, "Combined state and parameter estimation of lithium-ion battery with active current injection," *IEEE Trans. Power Electron.*, vol. 35, no. 4, pp. 4439–4447, Apr. 2020.
- [49] F. Naseri, E. Schaltz, D.-I. Stroe, A. Gismero, and E. Farjah, "An enhanced equivalent circuit model with real-time parameter identification for battery state-of-charge estimation," *IEEE Trans. Ind. Electron.*, vol. 69, no. 4, pp. 3743–3751, Apr. 2022.
- [50] S. Li, Z. Jiang, J. Han, Z. Xu, C. Wang, H. Huang, C. Yu, S.-J. Lee, P. Pianetta, H. Ohldag, J. Qiu, J.-S. Lee, F. Lin, K. Zhao, and Y. Liu, "Mutual modulation between surface chemistry and bulk microstructure within secondary particles of nickel-rich layered oxides," *Nature Commun.*, vol. 11, no. 1, pp. 1–9, Dec. 2020.
- [51] D. Di Domenico, G. Fiengo, and A. Stefanopoulou, "Lithium-ion battery state of charge estimation with a Kalman filter based on a electrochemical model," in *Proc. IEEE Int. Conf. Control Appl.*, Sep. 2008, pp. 702–707.
- [52] B. S. Haran, B. N. Popov, and R. E. White, "Determination of the hydrogen diffusion coefficient in metal hydrides by impedance spectroscopy," *J. Power Sources*, vol. 75, no. 1, pp. 56–63, Sep. 1998.
- [53] G. Ning and B. N. Popov, "Cycle life modeling of lithium-ion batteries," *J. Electrochem. Soc.*, vol. 151, no. 10, p. A1584, 2004.
- [54] S. Santhanagopalan, Q. Guo, P. Ramadass, and R. E. White, "Review of models for predicting the cycling performance of lithium ion batteries," *J. Power Sources*, vol. 156, no. 2, pp. 620–628, 2006.
- [55] S. J. Moura, F. B. Argomedo, R. Klein, A. Mirtabatabaei, and M. Krstic, "Battery state estimation for a single particle model with electrolyte dynamics," *IEEE Trans. Control Syst. Technol.*, vol. 25, no. 2, pp. 453–468, Mar. 2017.
- [56] I. Oyewole, K. H. Kwak, Y. Kim, and X. Lin, "Optimal discretization approach to the enhanced single-particle model for Li-ion batteries," *IEEE Trans. Transport. Electrific.*, vol. 7, no. 2, pp. 369–381, Jun. 2021.
- [57] D. Zhang, S. Dey, L. D. Couto, and S. J. Moura, "Battery adaptive observer for a single-particle model with intercalation-induced stress," *IEEE Trans. Control Syst. Technol.*, vol. 28, no. 4, pp. 1363–1377, Jul. 2020.
- [58] J. Li, K. Adewuyi, N. Lotfi, R. G. Landers, and J. Park, "A single particle model with chemical/mechanical degradation physics for lithium ion battery state of health (SOH) estimation," *Appl. Energy*, vol. 212, pp. 1178–1190, Feb. 2018.

- [59] M. Doyle and J. Newman, "The use of mathematical modeling in the design of lithium/polymer battery systems," *Electrochim. Acta*, vol. 40, nos. 13–14, pp. 2191–2196, Oct. 1995.
- [60] P. Ramadass, B. Haran, P. M. Gomadam, R. White, and B. N. Popov, "Development of first principles capacity fade model for li-ion cells," *J. Electrochem. Soc.*, vol. 151, no. 2, p. A196, 2004.
- [61] L. Zhang, Z. Wang, X. Hu, F. Sun, and D. G. Dorrell, "A comparative study of equivalent circuit models of ultracapacitors for electric vehicles," *J. Power Sources*, vol. 274, no. 8, pp. 899–906, 2015.
- [62] K.-T. Lee, M.-J. Dai, and C.-C. Chuang, "Temperature-compensated model for lithium-ion polymer batteries with extended Kalman filter state-of-charge estimation for an implantable charger," *IEEE Trans. Ind. Electron.*, vol. 65, no. 1, pp. 589–596, Jan. 2018.
- [63] L. H. J. Raijmakers, D. L. Danilov, J. P. M. V. Lammeren, T. J. G. Lammers, H. J. Bergveld, and P. H. L. Notten, "Non-zero intercept frequency: An accurate method to determine the integral temperature of Li-ion batteries," *IEEE Trans. Ind. Electron.*, vol. 63, no. 5, pp. 3168–3178, May 2016.
- [64] Y. Kim, S. Mohan, J. B. Siegel, A. G. Stefanopoulou, and Y. Ding, "The estimation of temperature distribution in cylindrical battery cells under unknown cooling conditions," *IEEE Trans. Control Syst. Technol.*, vol. 22, no. 6, pp. 2277–2286, Nov. 2014.
- [65] S. Shahid and M. Agelin-Chaab, "Development of hybrid thermal management techniques for battery packs," *Appl. Thermal Eng.*, vol. 186, Mar. 2021, Art. no. 116542.
- [66] Y. Li, Z. Wei, B. Xiong, and D. M. Vilathgamuwa, "Adaptive ensemble-based electrochemical–thermal degradation state estimation of lithium-ion batteries," *IEEE Trans. Ind. Electron.*, vol. 69, no. 7, pp. 6984–6996, Jul. 2022.
- [67] M. K. S. Verma, S. Basu, R. S. Patil, K. S. Hariharan, S. P. Adiga, S. M. Kolake, D. Oh, T. Song, and Y. Sung, "On-board state estimation in electrical vehicles: Achieving accuracy and computational efficiency through an electrochemical model," *IEEE Trans. Veh. Technol.*, vol. 69, no. 3, pp. 2563–2575, Mar. 2020.
- [68] J. Chiew, C. S. Chin, W. D. Toh, Z. Gao, J. Jia, and C. Zhang, "A pseudo three-dimensional electrochemical-thermal model of a cylindrical LiFePO<sub>4</sub>/graphite battery," *Appl. Thermal Eng.*, vol. 147, pp. 450–463, Jan. 2019.
- [69] M. A. Hannan, M. S. H. Lipu, A. Hussain, M. H. Saad, and A. Ayob, "Neural network approach for estimating state of charge of lithium-ion battery using backtracking search algorithm," *IEEE Access*, vol. 6, pp. 10069–10079, 2018.
- [70] D. N. How, M. A. Hannan, M. S. H. Lipu, K. S. Sahari, P. J. Ker, and K. M. Muttaqi, "State-of-charge estimation of Li-ion battery in electric vehicles: A deep neural network approach," *IEEE Trans. Ind. Appl.*, vol. 56, no. 5, pp. 5565–5574, Sep./Oct. 2020.
- [71] M. Zhu, Q. Ouyang, Y. Wan, and Z. Wang, "Remaining useful life prediction of lithium-ion batteries: A hybrid approach of grey-Markov chain model and improved Gaussian process," *IEEE J. Emerg. Sel. Topics Power Electron.*, early access, Jul. 19, 2021, doi: 10.1109/JESTPE.2021.3098378.
- [72] H. Chun, J. Kim, J. Yu, and S. Han, "Real-time parameter estimation of an electrochemical lithium-ion battery model using a long short-term memory network," *IEEE Access*, vol. 8, pp. 81789–81799, 2020.
- [73] X. Feng, C. Weng, X. He, X. Han, L. Lu, D. Ren, and M. Ouyang, "Online state-of-health estimation for Li-ion battery using partial charging segment based on support vector machine," *IEEE Trans. Veh. Technol.*, vol. 68, no. 9, pp. 8583–8592, Sep. 2019.
- [74] W. Huang, X. Feng, X. Han, W. Zhang, and F. Jiang, "Questions and answers relating to lithium-ion battery safety issues," *Cell Rep. Phys. Sci.*, vol. 2, no. 1, Jan. 2021, Art. no. 100285.
- [75] C. R. Birk, M. R. Roberts, E. McTurk, P. G. Bruce, and D. A. Howey, "Degradation diagnostics for lithium ion cells," *J. Power Sources*, vol. 341, pp. 373–386, Feb. 2017.
- [76] T. R. Jow, S. A. Delp, J. L. Allen, J.-P. Jones, and M. C. Smart, "Factors limiting Li<sup>+</sup> charge transfer kinetics in Li-ion batteries," *J. Electrochem. Soc.*, vol. 165, no. 2, p. A361, 2018.
- [77] C. Vidal, O. Gross, R. Gu, P. Kollmeyer, and A. Emadi, "xEV Li-ion battery low-temperature effects—Review," *IEEE Trans. Veh. Technol.*, vol. 68, no. 5, pp. 4560–4572, May 2019.
- [78] H. Karlsten, T. Dong, Z. Yang, and R. Carvalho, "Temperature-dependence in battery management systems for electric vehicles: Challenges, criteria, and solutions," *IEEE Access*, vol. 7, pp. 142203–142213, 2019.
- [79] S. Mohan, Y. Kim, and A. G. Stefanopoulou, "Energy-conscious warm-up of Li-ion cells from subzero temperatures," *IEEE Trans. Ind. Electron.*, vol. 63, no. 5, pp. 2954–2964, May 2016.
- [80] J. Jaguemont, L. Boulon, and Y. Dubé, "Characterization and modeling of a hybrid-electric-vehicle lithium-ion battery pack at low temperatures," *IEEE Trans. Veh. Technol.*, vol. 65, no. 1, pp. 1–14, Jan. 2016.
- [81] P. Keil, M. Englberger, and A. Jossen, "Hybrid energy storage systems for electric vehicles: An experimental analysis of performance improvements at subzero temperatures," *IEEE Trans. Veh. Technol.*, vol. 65, no. 3, pp. 998–1006, Mar. 2016.
- [82] Y. Shang, K. Liu, N. Cui, Q. Zhang, and C. Zhang, "A sine-wave heating circuit for automotive battery self-heating at subzero temperatures," *IEEE Trans. Ind. Informat.*, vol. 16, no. 5, pp. 3355–3365, May 2020.
- [83] J. Jaguemont, L. Boulon, P. Venet, Y. Dubé, and A. Sari, "Lithium-ion battery aging experiments at subzero temperatures and model development for capacity fade estimation," *IEEE Trans. Veh. Technol.*, vol. 65, no. 6, pp. 4328–4343, Jun. 2016.
- [84] S. Mohan, J. B. Siegel, A. G. Stefanopoulou, and R. Vasudevan, "An energy-optimal warm-up strategy for Li-ion batteries and its approximations," *IEEE Trans. Control Syst. Technol.*, vol. 27, no. 3, pp. 1165–1180, May 2019.
- [85] G. Sikha, B. N. Popov, and R. E. White, "Effect of porosity on the capacity fade of a lithium-ion battery," *J. Electrochem. Soc.*, vol. 151, no. 7, p. A1104, 2004.
- [86] L. Zhang, W. Fan, Z. Wang, W. Li, and D. U. Sauer, "Battery heating for lithium-ion batteries based on multi-stage alternative currents," *J. Energy Storage*, vol. 32, Dec. 2020, Art. no. 101885.
- [87] X. Hu, K. Zhang, K. Liu, X. Lin, S. Dey, and S. Onori, "Advanced fault diagnosis for lithium-ion battery systems: A review of fault mechanisms, fault features, and diagnosis procedures," *IEEE Ind. Electron. Mag.*, vol. 14, no. 3, pp. 65–91, Sep. 2020.
- [88] D. Ren, X. Feng, L. Lu, M. Ouyang, S. Zheng, J. Li, and X. He, "An electrochemical-thermal coupled overcharge-to-thermal-runaway model for lithium ion battery," *J. Power Sources*, vol. 364, pp. 328–340, Oct. 2017.
- [89] X. Lin, K. Khosravinia, X. Hu, J. Li, and W. Lu, "Lithium plating mechanism, detection, and mitigation in lithium-ion batteries," *Prog. Energy Combustion Sci.*, vol. 87, Nov. 2021, Art. no. 100953.
- [90] J. Zhang, L. Zhang, F. Sun, and Z. Wang, "An overview on thermal safety issues of lithium-ion batteries for electric vehicle application," *IEEE Access*, vol. 6, pp. 23848–23863, 2018.
- [91] G. Pistoia and B. Liaw, *Behaviour of Lithium-Ion Batteries in Electric Vehicles: Battery Health, Performance, Safety, and Cost*. Berlin, Germany: Springer, 2018.
- [92] Y. Cui, P. Zuo, C. Du, Y. Gao, J. Yang, X. Cheng, Y. Ma, and G. Yin, "State of health diagnosis model for lithium ion batteries based on real-time impedance and open circuit voltage parameters identification method," *Energy*, vol. 144, pp. 647–656, Feb. 2018.
- [93] K. S. Ng, C.-S. Moo, Y.-P. Chen, and Y.-C. Hsieh, "Enhanced Coulomb counting method for estimating state-of-charge and state-of-health of lithium-ion batteries," *Appl. Energy*, vol. 86, no. 9, pp. 1506–1511, Sep. 2009.
- [94] E. R. Wognsen, B. R. Haverkort, M. Jongerden, R. R. Hansen, and K. G. Larsen, "A score function for optimizing the cycle-life of battery-powered embedded systems," in *Proc. Int. Conf. Formal Modeling Anal. Timed Syst.* Cham, Switzerland: Springer, 2015, pp. 305–320.
- [95] P. Shen, M. Ouyang, L. Lu, J. Li, and X. Feng, "The co-estimation of state of charge, state of health, and state of function for lithium-ion batteries in electric vehicles," *IEEE Trans. Veh. Technol.*, vol. 67, no. 1, pp. 92–103, Jan. 2018.
- [96] D. Liu, X. Yin, Y. Song, W. Liu, and Y. Peng, "An on-line state of health estimation of lithium-ion battery using unscented particle filter," *IEEE Access*, vol. 6, pp. 40990–41001, 2018.
- [97] C. She, L. Zhang, Z. Wang, F. Sun, P. Liu, and C. Song, "Battery state of health estimation based on incremental capacity analysis method: Synthesizing from cell-level test to real-world application," *IEEE J. Emerg. Sel. Topics Power Electron.*, early access, Sep. 14, 2022, doi: 10.1109/JESTPE.2021.3112754.
- [98] W. Yan, B. Zhang, G. Zhao, S. Tang, G. Niu, and X. Wang, "A battery management system with a Lebesgue-sampling-based extended Kalman filter," *IEEE Trans. Ind. Electron.*, vol. 66, no. 4, pp. 3227–3236, Apr. 2019.
- [99] M. Ahwiadi and W. Wang, "An enhanced mutated particle filter technique for system state estimation and battery life prediction," *IEEE Trans. Instrum. Meas.*, vol. 68, no. 3, pp. 923–935, Mar. 2019.

- [100] S. Rahimifard, R. Ahmed, and S. Habibi, "Interacting multiple model strategy for electric vehicle batteries state of charge/health/power estimation," *IEEE Access*, vol. 9, pp. 109875–109888, 2021.
- [101] Y. Jiang, J. Zhang, L. Xia, and Y. Liu, "State of health estimation for lithium-ion battery using empirical degradation and error compensation models," *IEEE Access*, vol. 8, pp. 123858–123868, 2020.
- [102] A. Thingvad, L. Calearo, P. B. Andersen, and M. Marinelli, "Empirical capacity measurements of electric vehicles subject to battery degradation from V2G services," *IEEE Trans. Veh. Technol.*, vol. 70, no. 8, pp. 7547–7557, Aug. 2021.
- [103] Y. Zheng, Y. Cui, X. Han, and M. Ouyang, "A capacity prediction framework for lithium-ion batteries using fusion prediction of empirical model and data-driven method," *Energy*, vol. 237, Dec. 2021, Art. no. 121556.
- [104] J. Wang, P. Liu, J. Hicks-Garner, E. Sherman, S. Soukiazian, M. Verbrugge, H. Tataria, J. Musser, and P. Finamore, "Cycle-life model for graphite-LiFePO<sub>4</sub> cells," *J. Power Sources*, vol. 196, no. 8, pp. 3942–3948, Apr. 2011.
- [105] J. Qu, F. Liu, Y. Ma, and J. Fan, "A neural-network-based method for RUL prediction and SOH monitoring of lithium-ion battery," *IEEE Access*, vol. 7, pp. 87178–87191, 2019.
- [106] J.-H. Lee, H.-S. Kim, and I.-S. Lee, "Deep neural network based SOH monitoring of battery module," in *Proc. IEEE Eurasia Conf. IoT, Commun. Eng. (ECICE)*, Oct. 2019, pp. 14–16.
- [107] C.-M. Lai and T.-J. Kuo, "Available capacity computation model based on long short-term memory recurrent neural network for gelled-electrolyte batteries in golf carts," *IEEE Access*, vol. 10, pp. 54433–54444, 2022.
- [108] H. Dai, G. Zhao, M. Lin, J. Wu, and G. Zheng, "A novel estimation method for the state of health of lithium-ion battery using prior knowledge-based neural network and Markov chain," *IEEE Trans. Ind. Electron.*, vol. 66, no. 10, pp. 7706–7716, Oct. 2019.
- [109] N. Khan, F. U. M. Ullah, Afnan, A. Ullah, M. Y. Lee, and S. W. Baik, "Batteries state of health estimation via efficient neural networks with multiple channel charging profiles," *IEEE Access*, vol. 9, pp. 7797–7813, 2021, doi: [10.1109/ACCESS.2020.3047732](https://doi.org/10.1109/ACCESS.2020.3047732).
- [110] H. Chaoui and C. C. Ibe-Ekeocha, "State of charge and state of health estimation for lithium batteries using recurrent neural networks," *IEEE Trans. Veh. Technol.*, vol. 66, no. 10, pp. 8773–8783, Oct. 2017.
- [111] R. R. Richardson, C. R. Birk, M. A. Osborne, and D. A. Howey, "Gaussian process regression for in situ capacity estimation of lithium-ion batteries," *IEEE Trans. Ind. Informat.*, vol. 15, no. 1, pp. 127–138, Jan. 2019.
- [112] K. Liu, X. Hu, H. Zhou, L. Tong, W. D. Widanage, and J. Marco, "Feature analyses and modeling of lithium-ion battery manufacturing based on random forest classification," *IEEE/ASME Trans. Mechatronics*, vol. 26, no. 6, pp. 2944–2955, Dec. 2021.
- [113] J. Tian, R. Xiong, W. Shen, J. Lu, and X.-G. Yang, "Deep neural network battery charging curve prediction using 30 points collected in 10 min," *Joule*, vol. 5, no. 6, pp. 1521–1534, Jun. 2021.
- [114] X. Hu, D. Cao, and B. Egardt, "Condition monitoring in advanced battery management systems: Moving horizon estimation using a reduced electrochemical model," *IEEE/ASME Trans. Mechatronics*, vol. 23, no. 1, pp. 167–178, Feb. 2018.
- [115] P. A. Topan, M. N. Ramadan, G. Fathoni, A. I. Cahyadi, and O. Wahyunggoro, "State of charge (SOC) and state of health (SOH) estimation on lithium polymer battery via Kalman filter," in *Proc. 2nd Int. Conf. Sci. Technol.-Comput. (ICST)*, Oct. 2016, pp. 93–96.
- [116] X. Hu, H. Yuan, C. Zou, Z. Li, and L. Zhang, "Co-estimation of state of charge and state of health for lithium-ion batteries based on fractional-order calculus," *IEEE Trans. Veh. Technol.*, vol. 67, no. 11, pp. 10319–10329, Nov. 2018.
- [117] J. Liu and Z. Chen, "Remaining useful life prediction of lithium-ion batteries based on health indicator and Gaussian process regression model," *IEEE Access*, vol. 7, pp. 39474–39484, 2019.
- [118] A. K. Severson, M. P. Attia, N. Jin, N. Perkins, B. Jiang, Z. Yang, M. H. Chen, M. Aykol, P. K. Herring, D. Fragedakis, M. Z. Bazant, S. J. Harris, W. C. Chueh, and R. D. Braatz, "Data-driven prediction of battery cycle life before capacity degradation," *Nature Energy*, vol. 4, no. 5, pp. 383–391, May 2019.
- [119] R. Zhou, S. Fu, and W. Peng, "A review of state-of-health estimation of lithium-ion batteries: Experiments and data," in *Proc. Asia-Pacific Int. Symp. Adv. Rel. Maintenance Model. (APARM)*, Aug. 2020, pp. 1–6.
- [120] X. Zhang, Y. Han, and W. Zhang, "A review of factors affecting the lifespan of lithium-ion battery and its health estimation methods," *Trans. Electr. Electron. Mater.*, vol. 22, pp. 567–574, Jul. 2021.
- [121] Z. Wang, C. Song, L. Zhang, Y. Zhao, P. Liu, and D. G. Dorrell, "A data-driven method for battery charging capacity abnormality diagnosis in electric vehicle applications," *IEEE Trans. Transport. Electrific.*, vol. 8, no. 1, pp. 990–999, Mar. 2022.
- [122] A. Bonfitto, E. Ezemobi, N. Amati, S. Feraco, A. Tonoli, and S. Hegde, "State of health estimation of lithium batteries for automotive applications with artificial neural networks," in *Proc. AEIT Int. Conf. Electr. Electron. Technol. Automot. (AEIT AUTOMOTIVE)*, Jul. 2019, pp. 1–5.
- [123] Y. Choi, S. Ryu, K. Park, and H. Kim, "Machine learning-based lithium-ion battery capacity estimation exploiting multi-channel charging profiles," *IEEE Access*, vol. 7, pp. 75143–75152, 2019.
- [124] G.-W. You, S. Park, and D. Oh, "Real-time state-of-health estimation for electric vehicle batteries: A data-driven approach," *Appl. Energy*, vol. 176, pp. 92–103, Aug. 2016.
- [125] J. Tian, R. Xiong, and W. Shen, "State-of-health estimation based on differential temperature for lithium ion batteries," *IEEE Trans. Power Electron.*, vol. 35, no. 10, pp. 10363–10373, Oct. 2020.
- [126] Z. Chen, M. Sun, X. Shu, R. Xiao, and J. Shen, "Online state of health estimation for lithium-ion batteries based on support vector machine," *Appl. Sci.*, vol. 8, no. 6, p. 925, Jun. 2018.
- [127] H. Pan, Z. Lü, H. Wang, H. Wei, and L. Chen, "Novel battery state-of-health online estimation method using multiple health indicators and an extreme learning machine," *Energy*, vol. 160, pp. 466–477, Oct. 2018.
- [128] Y. Li, C. F. Zou, M. Berecibar, E. E. Nanini, J. C. W. Chan, P. van den Bossche, J. Van Mierlo, and N. Omar, "Random forest regression for online capacity estimation of lithium-ion batteries," *Appl. Energy, Article*, vol. 232, pp. 197–210, Dec. 2018.
- [129] Y. Duan, J. Tian, J. Lu, C. Wang, W. Shen, and R. Xiong, "Deep neural network battery impedance spectra prediction by only using constant-current curve," *Energy Storage Mater.*, vol. 41, pp. 24–31, Oct. 2021.
- [130] J. Tian, R. Xiong, W. Shen, and F. Sun, "Electrode ageing estimation and open circuit voltage reconstruction for lithium ion batteries," *Energy Storage Mater.*, vol. 37, pp. 283–295, May 2021.
- [131] B. Saha and K. Goebel, "Battery data set," NASA Ames Prognostics Data Repository, 2007. [Online]. Available: <http://ti.arc.nasa.gov/project/prognostic-data-repository>
- [132] W. He, N. Williard, M. Osterman, and M. Pecht, "Prognostics of lithium-ion batteries based on Dempster-Shafer theory and the Bayesian Monte Carlo method," *J. Power Sources*, vol. 196, pp. 10314–10321, Dec. 2011.
- [133] C. Birk, "Oxford battery degradation dataset 1," Univ. Oxford, Oxford, U.K., 2017.
- [134] J. Wu, C. Zhang, and Z. Chen, "An online method for lithium-ion battery remaining useful life estimation using importance sampling and neural networks," *Appl. Energy*, vol. 173, pp. 134–140, Jul. 2016.
- [135] H. Chaoui, N. Golbon, I. Hmouz, R. Souissi, and S. Tahar, "Lyapunov-based adaptive state of charge and state of health estimation for lithium-ion batteries," *IEEE Trans. Ind. Electron.*, vol. 62, no. 3, pp. 1610–1618, Mar. 2015.
- [136] V. Ramadesigan, K. Chen, N. A. Burns, V. Boovaragavan, R. D. Braatz, and V. R. Subramanian, "Parameter estimation and capacity fade analysis of lithium-ion batteries using reformulated models," *J. Electrochim. Soc.*, vol. 158, no. 9, p. A1048, 2011.
- [137] G. Lenze, F. Röder, H. Bockholt, W. Haselrieder, A. Kwade, and U. Kreuer, "Simulation-supported analysis of calendering impacts on the performance of lithium-ion-batteries," *J. Electrochim. Soc.*, vol. 164, no. 6, p. A1223, 2017.
- [138] H. Chun and S. Han, "Electrochemical model parameter estimation of a lithium-ion battery using a metaheuristic algorithm: Cascaded improved harmony search," *IFAC-PapersOnLine*, vol. 51, no. 28, pp. 409–413, 2018.
- [139] V. Laue, F. Röder, and U. Kreuer, "Practical identifiability of electrochemical P2D models for lithium-ion batteries," *J. Appl. Electrochim.*, vol. 51, no. 9, pp. 1253–1265, Sep. 2021.
- [140] Z. Cui, N. Cui, C. Wang, C. Li, and C. Zhang, "A robust online parameter identification method for lithium-ion battery model under asynchronous sampling and noise interference," *IEEE Trans. Ind. Electron.*, vol. 68, no. 10, pp. 9550–9560, Oct. 2021.
- [141] Y. Li, B. Xiong, D. M. Vilathgamuwa, Z. Wei, C. Xie, and C. Zou, "Constrained ensemble Kalman filter for distributed electrochemical state estimation of lithium-ion batteries," *IEEE Trans. Ind. Informat.*, vol. 17, no. 1, pp. 240–250, Jan. 2021.
- [142] J. Li, R. G. Landers, and J. Park, "A comprehensive single-particle-degradation model for battery state-of-health prediction," *J. Power Sources*, vol. 456, Apr. 2020, Art. no. 227950.

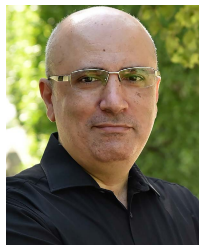
- [143] J. Sihvo, T. Roinila, and D.-I. Stroe, "Novel fitting algorithm for parametrization of equivalent circuit model of li-ion battery from broadband impedance measurements," *IEEE Trans. Ind. Electron.*, vol. 68, no. 6, pp. 4916–4926, Jun. 2021.
- [144] A. Guha and A. Patra, "Online estimation of the electrochemical impedance spectrum and remaining useful life of lithium-ion batteries," *IEEE Trans. Instrum. Meas.*, vol. 67, no. 8, pp. 1836–1849, Aug. 2018.
- [145] D. Zhang, S. Dey, H. E. Perez, and S. J. Moura, "Remaining useful life estimation of lithium-ion batteries based on thermal dynamics," in *Proc. Amer. Control Conf. (ACC)*, May 2017, pp. 4042–4047.
- [146] G. Dong, Z. Chen, J. Wei, and Q. Ling, "Battery health prognosis using Brownian motion modeling and particle filtering," *IEEE Trans. Ind. Electron.*, vol. 65, no. 11, pp. 8646–8655, Nov. 2018.
- [147] Y. Zhang, Y. Yang, X. Xiu, H. Li, and R. Liu, "A remaining useful life prediction method in the early stage of stochastic degradation process," *IEEE Trans. Circuits Syst. II, Exp. Briefs*, vol. 68, no. 6, pp. 2027–2031, Jun. 2021.
- [148] T. Li, H. Pei, Z. Pang, X. Si, and J. Zheng, "A sequential Bayesian updated Wiener process model for remaining useful life prediction," *IEEE Access*, vol. 8, pp. 5471–5480, 2020.
- [149] S. Ansari, A. Ayob, M. S. H. Lipu, M. H. M. Saad, and A. Hussain, "A comparative analysis of lithium ion battery input profiles for remaining useful life prediction by cascade forward neural network," in *Proc. IEEE World AI IoT Congr. (AIoT)*, May 2021, pp. 181–186.
- [150] P. Shrivastava, T. K. Soon, M. Y. B. Idris, S. Mekhilef, and S. B. R. S. Adnan, "Lithium-ion battery state of energy estimation using deep neural network and support vector regression," in *Proc. IEEE 12th Energy Convers. Congr. Expo. Asia (ECCE-Asia)*, May 2021, pp. 2175–2180.
- [151] M. S. Hosen, J. Jaguemont, J. Van Mierlo, and M. Berecibar, "Battery lifetime prediction and performance assessment of different modeling approaches," *iScience*, vol. 24, no. 2, Feb. 2021, Art. no. 102060.
- [152] L. Cui, X. Wang, H. Wang, and J. Ma, "Research on remaining useful life prediction of rolling element bearings based on time-varying Kalman filter," *IEEE Trans. Instrum. Meas.*, vol. 69, no. 6, pp. 2858–2867, Jun. 2020.
- [153] G. Dong, J. Wei, Z. Chen, H. Sun, and X. Yu, "Remaining dischargeable time prediction for lithium-ion batteries using unscented Kalman filter," *J. Power Sources*, vol. 364, pp. 316–327, Oct. 2017.
- [154] L. Yan, J. Peng, D. Gao, Y. Wu, Y. Liu, H. Li, W. Liu, and Z. Huang, "A hybrid method with cascaded structure for early-stage remaining useful life prediction of lithium-ion battery," *Energy*, vol. 243, Mar. 2022, Art. no. 123038.
- [155] V. Sangwan, R. Kumar, and A. K. Rathore, "An empirical capacity degradation modeling and prognostics of remaining useful life of Li-ion battery using unscented Kalman filter," in *Proc. 8th IEEE India Int. Conf. Power Electron. (IICPE)*, Dec. 2018, pp. 1–6.
- [156] B. Saha, K. Goebel, S. Poll, and J. Christophersen, "Prognostics methods for battery health monitoring using a Bayesian framework," *IEEE Trans. Instrum. Meas.*, vol. 58, no. 2, pp. 291–296, Feb. 2009.
- [157] D. A. Pola, H. F. Navarrete, M. E. Orchard, R. S. Rabié, M. A. Cerda, B. E. Olivares, J. F. Silva, P. A. Espinoza, and A. Pérez, "Particle-filtering-based discharge time prognosis for lithium-ion batteries with a statistical characterization of use profiles," *IEEE Trans. Rel.*, vol. 64, no. 2, pp. 710–720, Jun. 2015.
- [158] X. Tang, K. Liu, X. Wang, B. Liu, F. Gao, and W. D. Widanage, "Real-time aging trajectory prediction using a base model-oriented gradient-correction particle filter for lithium-ion batteries," *J. Power Sources*, vol. 440, Nov. 2019, Art. no. 227118.
- [159] M. Ahwidi and W. Wang, "An enhanced particle filter technology for battery system state estimation and RUL prediction," *Measurement*, vol. 191, Mar. 2022, Art. no. 110817.
- [160] L. Zhang, Z. Mu, and C. Sun, "Remaining useful life prediction for lithium-ion batteries based on exponential model and particle filter," *IEEE Access*, vol. 6, pp. 17729–17740, 2018.
- [161] K. Liu, K. Li, Q. Peng, and C. Zhang, "A brief review on key technologies in the battery management system of electric vehicles," *Frontiers Mech. Eng.*, vol. 14, no. 1, pp. 47–64, 2019.
- [162] B. Long, W. Xian, L. Jiang, and Z. Liu, "An improved autoregressive model by particle swarm optimization for prognostics of lithium-ion batteries," *Microelectron. Rel.*, vol. 53, no. 6, pp. 821–831, 2013.
- [163] B. Gou, Y. Xu, and X. Feng, "State-of-health estimation and remaining-useful-life prediction for lithium-ion battery using a hybrid data-driven method," *IEEE Trans. Veh. Technol.*, vol. 69, no. 10, pp. 10854–10867, Oct. 2020.
- [164] H. Chaoqui, C. C. Ibe-Ekeocha, and H. Gualous, "Aging prediction and state of charge estimation of a LiFePO<sub>4</sub> battery using input time-delayed neural networks," *Electr. Power Syst. Res.*, vol. 146, pp. 189–197, May 2017.
- [165] M. Catelani, L. Ciani, R. Fantacci, G. Patrizi, and B. Picano, "Remaining useful life estimation for prognostics of lithium-ion batteries based on recurrent neural network," *IEEE Trans. Instrum. Meas.*, vol. 70, pp. 1–11, 2021.
- [166] K. Park, Y. Choi, W. J. Choi, H.-Y. Ryu, and H. Kim, "LSTM-based battery remaining useful life prediction with multi-channel charging profiles," *IEEE Access*, vol. 8, pp. 20786–20798, 2020.
- [167] H. Miao, B. Li, C. Sun, and J. Liu, "Joint learning of degradation assessment and RUL prediction for aeroengines via dual-task deep LSTM networks," *IEEE Trans. Ind. Informat.*, vol. 15, no. 9, pp. 5023–5032, Sep. 2019.
- [168] Z. Shi and A. Chehade, "A dual-LSTM framework combining change point detection and remaining useful life prediction," *Rel. Eng. Syst. Saf.*, vol. 205, Jan. 2021, Art. no. 107257.
- [169] M. Ma and Z. Mao, "Deep-convolution-based LSTM network for remaining useful life prediction," *IEEE Trans. Ind. Informat.*, vol. 17, no. 3, pp. 1658–1667, Mar. 2021.
- [170] J. Li, X. Li, and D. He, "A directed acyclic graph network combined with CNN and LSTM for remaining useful life prediction," *IEEE Access*, vol. 7, pp. 75464–75475, 2019.
- [171] J. Kim, S. Lee, and B. H. Cho, "Complementary cooperation algorithm based on DEKF combined with pattern recognition for SOC/capacity estimation and SOH prediction," *IEEE Trans. Power Electron.*, vol. 27, no. 1, pp. 436–451, Jan. 2012.
- [172] G. Dong, W. Han, and Y. Wang, "Dynamic Bayesian network-based lithium-ion battery health prognosis for electric vehicles," *IEEE Trans. Ind. Electron.*, vol. 68, no. 11, pp. 10949–10958, Nov. 2021.
- [173] A. Aitio and D. A. Howey, "Predicting battery end of life from solar off-grid system field data using machine learning," *Joule*, vol. 5, no. 12, pp. 3204–3220, Dec. 2021.
- [174] K. Liu, Y. Shang, Q. Ouyang, and W. D. Widanage, "A data-driven approach with uncertainty quantification for predicting future capacities and remaining useful life of lithium-ion battery," *IEEE Trans. Ind. Electron.*, vol. 68, no. 4, pp. 3170–3180, Apr. 2021.
- [175] K. Goebel, B. Saha, A. Saxena, J. R. Celaya, and J. P. Christophersen, "Prognostics in battery health management," *IEEE Instrum. Meas. Mag.*, vol. 11, no. 4, pp. 33–40, Aug. 2008.
- [176] X. Hu, Y. Che, X. Lin, and Z. Deng, "Health prognosis for electric vehicle battery packs: A data-driven approach," *IEEE/ASME Trans. Mechatronics*, vol. 25, no. 6, pp. 2622–2632, Dec. 2020.
- [177] R. R. Richardson, M. A. Osborne, and D. A. Howey, "Gaussian process regression for forecasting battery state of health," *J. Power Sources*, vol. 357, pp. 209–219, Jul. 2017.
- [178] R. R. Richardson, M. A. Osborne, and D. A. Howey, "Battery health prediction under generalized conditions using a Gaussian process transition model," *J. Energy Storage*, vol. 23, pp. 320–328, Jun. 2019.
- [179] J. Zhao, L. Chen, W. Pedrycz, and W. Wang, "Variational inference-based automatic relevance determination kernel for embedded feature selection of noisy industrial data," *IEEE Trans. Ind. Electron.*, vol. 66, no. 1, pp. 416–428, Jan. 2019.
- [180] M. E. Tipping, "The relevance vector machine," in *Proc. Adv. Neural Inf. Process. Syst.*, 2000, pp. 652–658.
- [181] M. E. Tipping, "Sparse Bayesian learning and the relevance vector machine," *J. Mach. Learn. Res.*, vol. 1, pp. 211–244, Sep. 2001.
- [182] H. Li, D. Pan, and C. L. P. Chen, "Intelligent prognostics for battery health monitoring using the mean entropy and relevance vector machine," *IEEE Trans. Syst., Man, Cybern., Syst.*, vol. 44, no. 7, pp. 851–862, Jul. 2014.
- [183] D. Liu, J. Zhou, D. Pan, Y. Peng, and X. Peng, "Lithium-ion battery remaining useful life estimation with an optimized relevance vector machine algorithm with incremental learning," *Measurement*, vol. 63, pp. 143–151, Mar. 2015.
- [184] M. Wei, M. Ye, J. B. Li, Q. Wang, and X. Xu, "State of charge estimation of lithium-ion batteries using LSTM and NARX neural networks," *IEEE Access*, vol. 8, pp. 189236–189245, 2020.



**MOHAMED ELMALLAWY** received the B.Sc. degree (Hons.) in electronics and communications engineering from the Higher Institute of Engineering, El Shorouk City, Egypt, in 2012, and the M.Sc. degree from the University of Rostock, Germany, in 2019. He is currently pursuing the Ph.D. degree with the Department of Computer Science, Missouri University of Science and Technology, Rolla, MO, USA. He is also a Former Graduate Research Assistant with the Department of Electrical and Computer Engineering, Tennessee Technological University, Cookeville, TN, USA. His research interests include machine learning, federated learning, satellite communication, wireless sensor networks, and multi-objective optimization with a focus on lithium-ion battery lifespan prediction and extension for electric vehicles.



**ALI ALOUANI** (Senior Member, IEEE) received the Diplome d’Ingenieur Principal from the l’Ecole Nationale d’Ingénieurs de Tunis, Tunisia, in 1981, and the Ph.D. degree in electrical and computer engineering (ECE) from the University of Tennessee, Knoxville, TN, USA, in 1986. He is currently a Professor of ECE at Tennessee Technological University. He has published 227 journals and conference papers. He is the holder of ten U.S. patents. His research interests include intelligent systems design, target tracking, sensor data fusion, monitoring and control of smart grid, and application of signal processing to medical diagnosis. He is a member of several professional societies. He was listed in Marquis Who’s Who in American Education and in Sciences and Engineering.



**TAREK ELFOLY** (Senior Member, IEEE) received the D.E.A. and Ph.D. degrees from the University of Franche Comte in France, in 1996 and 2000, respectively. He worked as an Assistant Professor at Ain Shams University, Cairo, Egypt, before joining Qatar University. He is currently an Associate Professor at Tennessee Technological University, USA. He has over ten years of experience in computer network research. He published over 60 articles, more than half of them are related to wireless sensing and network security. He supervised many post graduate students and served as an examiner for many others. He has many projects under development related to assistive technologies for people with disabilities. His projects won many national and regional awards. His research interests include network security and protocols, physical layer security, and wireless sensor networks especially in the field of structural health monitoring and health applications.



**AHMED M. MASSOUD** (Senior Member, IEEE) received the B.Sc. (Hons.) and M.Sc. degrees in electrical engineering from Alexandria University, Egypt, in 1997 and 2000, respectively, and the Ph.D. degree in electrical engineering from Heriot-Watt University, Edinburgh, U.K., in 2004. He is currently the Associate Dean for Research and Graduate Studies at the College of Engineering, Qatar University, Qatar, and a Professor at the Department of Electrical Engineering, College of Engineering, Qatar University. He supervised several M.Sc. and Ph.D. students at Qatar University. He holds 12 U.S. patents. He published more than 130 journal articles in the fields of power electronics, energy conversion, and power quality. His research interests include power electronics, energy conversion, renewable energy, and power quality. He has been awarded several research grants addressing research areas, such as energy storage systems, renewable energy sources, HVDC systems, electric vehicles, pulsed power applications, and power electronics for aerospace applications.